Electronic Supplementary Information

Bispidine as a β-strand nucleator: from a β-arch to self-assembled cages and vesicles

Hanuman Singh[a], Akshay Chenna[b], Upanshu Gangwar[a], Julie Borah[b], Gaurav Goel*[b], V. Haridas*[a]

[a]Department of Chemistry, Indian Institute of Technology Delhi, Hauz Khas, New Delhi-110016, India.

E-mail: haridasv@chemistry.iitd.ac.in

[b]Department of Chemical Engineering, Indian Institute of Technology Delhi, Hauz Khas, New Delhi-110016, India.

E-mail: goelg@chemical.iitd.ac.in

Experimental method

Reagents were purchased from Sigma-Aldrich, USA or Alfa Aesar (India). All the chemical reactions were monitored by thin-layer chromatography (TLC) using silica gel plates (Merck USA). Compounds were purified by silica gel (100−200 and 60-120 mesh) column chromatography. The solvents used were dried by standard methods. Infrared spectra were recorded on a Perkin Elmer spectrum IR, version 10.6.0 using KBr pellets. Characterizations were done by ^{1}H NMR, ^{13}C NMR, IR, and high-resolution mass spectrometry (HRMS). ^{1}H and ^{13}C NMR spectra were recorded on a Bruker-DPX- 300MHz and Bruker 500 MHz spectrometers, and the chemical shifts were reported relative to tetramethylsilane as the reference. Circular Dichroism (CD) spectra were recorded on AVIV model 410 spectropolarimeter equipped with a temperature controller. Mass spectra (HRMS) were recorded on a Bruker MicrO-TOF-QII model using ESI technique. Melting points were recorded by a Fisher scientific melting point apparatus. X-ray diffraction analysis was carried out on a Rigaku Oxford Diffraction with SuperNova (Mo) X-ray Source diffraction source. Structure solution, refinement, and data output were carried out with the ShelXTL (Sheldrick, 2015).

Scheme S1: Synthetic scheme for the bispidine-based peptides.

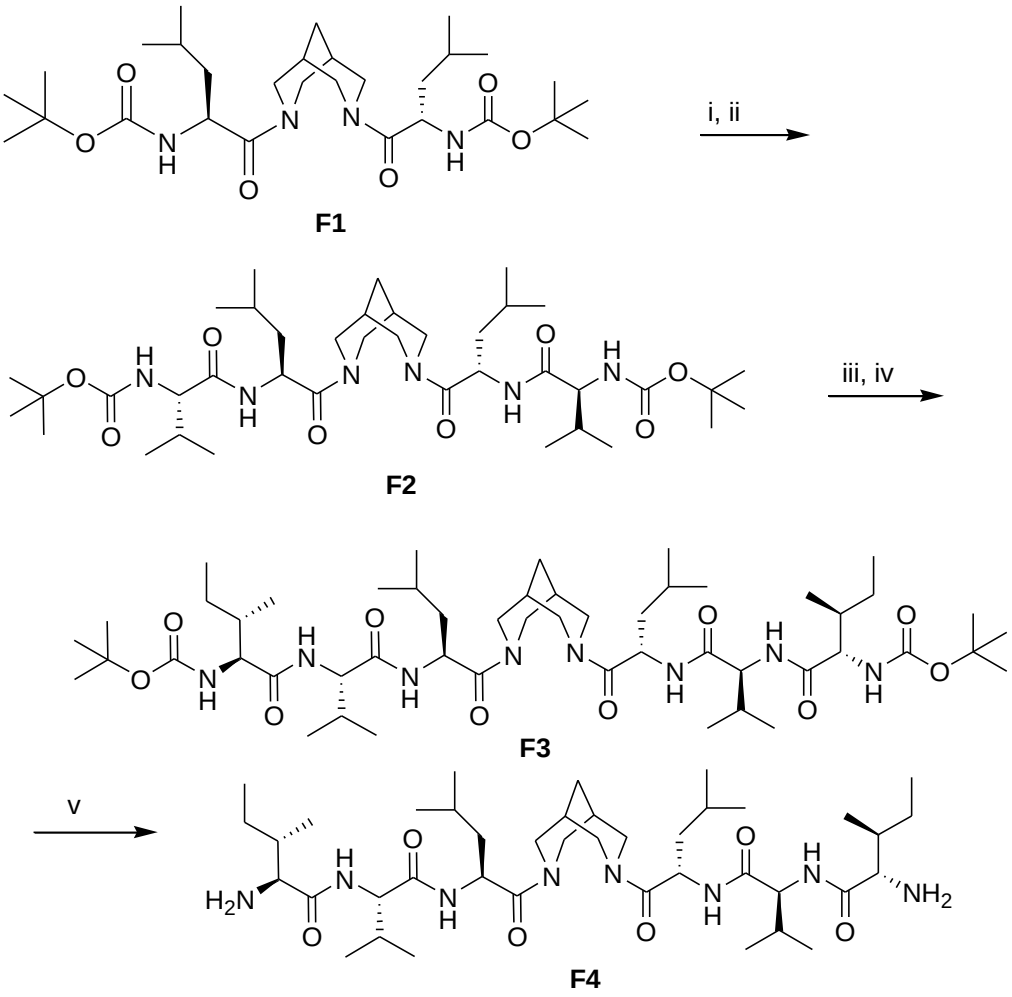

Reagents: (i) 25% TFA in dichloromethane; (ii) Boc-Val-OH, NHS, DCC, NEt_3; (iii) 25% TFA in dichloromethane; (iv) Boc-Ile-OH, NHS, DCC, NEt_3; (v) EtOAc.HCl.

Scheme S2: Synthesis of **F5**.

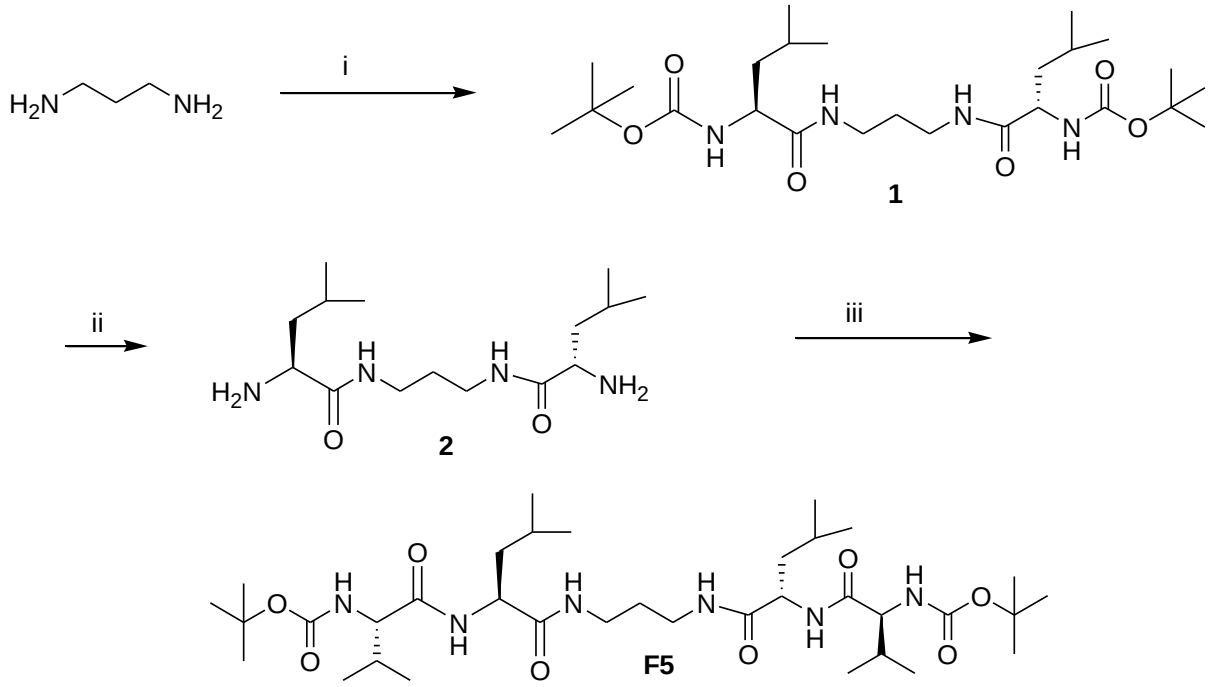

Reagents: (i) Boc-Leu-OH, NHS, DCC, NEt_3; (ii) 25% TFA in dichloromethane; (iii) Boc-Val-OH, NHS, DCC, NEt_3.

Scheme S3: Synthesis of **F6**.

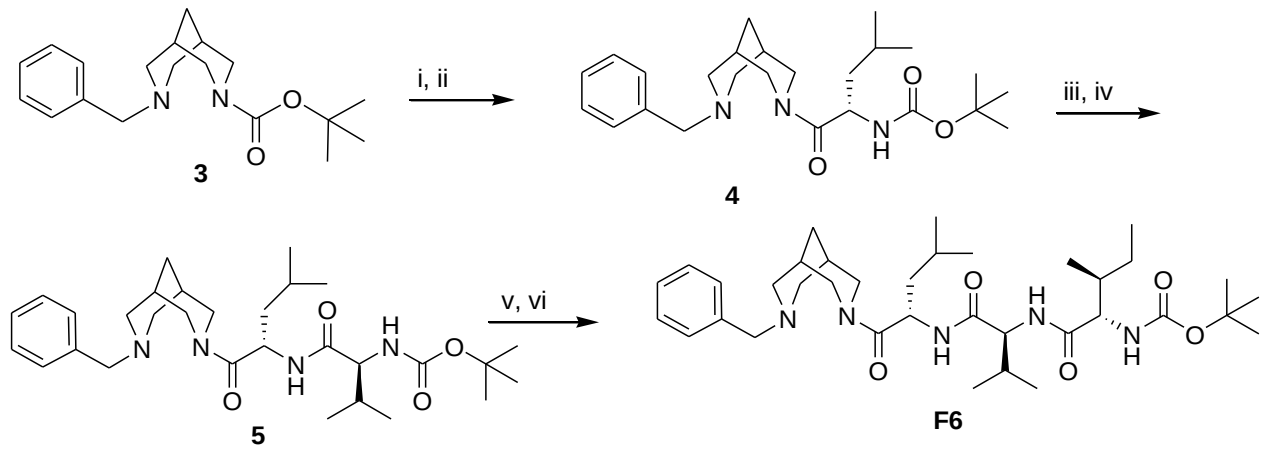

Reagents: (i) 25% TFA in dichloromethane; (ii) Boc-Leu-OH, NHS, DCC, NEt_3; (iii) 25% TFA in dichloromethane; (iv) Boc-Val-OH, NHS, DCC, NEt_3; (v) 25% TFA in dichloromethane; (vi) Boc-Ile-OH, NHS, DCC, NEt_3.

Synthesis of F1[1]

Synthesis of F2

To a well stirred and ice cooled solution of **F1** (0.350 g, 0.634 mmol) in dichloromethane (DCM) (10 mL) was added trifluoroacetic acid (TFA) (1.94 mL, 25.36 mmol), and the reaction mixture was stirred for 4h at room temperature. The reaction mixture was evaporated and used as such for further reaction.

The obtained amine was added to the DCM solution containing tert-butyloxy carbonyl (Boc) protected valine (0.275 g, 1.267 mmol), N-hydroxysuccinimide (NHS) (0.174 g, 1.520 mmol), N,N'-Dicyclohexylcarbodiimide (DCC) (0.311 g, 1.520 mmol) and triethylamine (NEt_3) (0.21 mL, 1.520 mmol). The resultant solution was stirred for 24h at room temperature. After completion of the reaction, the reaction mixture was evaporated and re-dissolved in ethyl acetate and filtered. The filtrate was washed with 0.2N H_2SO_4, saturated aq. $NaHCO_3$ and water. The organic layer was collected and dried over anhyd. Na_2SO_4 and evaporated under vacuum to obtain the crude product, and was purified by silica gel column chromatography (Ethyl acetate/Hexane in 6:4) to obtain 0.376 g of **F2** as solid.

Yield: 79%, Mp: 170 -172 ^oC.

^1H NMR (500 MHz, $CDCl_3$) δ: 0.85 (m, minor), 0.89 (d, *J* = 7 Hz, 6H), 0.91 (d, *J* = 6.5 Hz, 6H), 0.93 (d, *J* = 6.5 Hz, 6H), 0.96 (d, *J* = 6.5 Hz, minor), 1.00 (d, *J* = 6.5 Hz, 6H), 1.25 (m, 2H), 1.43 (s+m, 20H), 1.62 (m, 2H), 1.88 (br s, 2H), 2.07 (m, 2H), 2.13 (br s, 2H), 2.88 (d, *J* = 14 Hz, minor), 2.94 (d, *J* = 13.5 Hz, 2H), 3.29 (d, *J* = 12.5 Hz, minor), 3.41 (d, *J* = 12.5 Hz, 2H), 3.84 (d, *J* = 13 Hz, , 2H), 3.90 (m, 2H), 3.98 (minor), 4.48 (d, *J*= 14 Hz, 2H), 4.53 (d, *J*

= 14.5 Hz, minor), 4.80 (minor), 4.90 (t, *J* = 9 Hz, 2H), 5.05 (d, *J* = 9 Hz, 2H), 5.37 (d, *J* = 9 Hz, minor), 6.55 (d, *J* = 8 Hz, 2H), 7.04 (br d, minor); ^{13}C NMR (75 MHz, $CDCl_3$) δ: 17.7, 19.3, 21.4, 23.6, 24.7, 27.4, 28.3, 29.9, 30.9, 43.5, 46.8, 47.0, 49.8, 60.0, 79.8, 155.8, 171.3, 172.1; IR (KBr): 3439, 3319, 2962, 2930, 2870, 1709, 1633, 1523, 1453, 1389, 1366, 1246, 1171, 1093; HRMS calcd. for $C_{39}H_{70}N_6NaO_8$ m/z 773.5147, found m/z 773.5128.

Synthesis of F3

To a well stirred and ice cooled solution of compound **F2** (0.250 g, 0.333 mmol) in DCM (10 mL) was added TFA (1.01 mL, 13.32 mmol), and the reaction mixture was stirred for 4h at room temperature. The reaction mixture was evaporated and used as such for further reaction. The obtained amine was added to the DCM solution of Boc-isoleucine (0.153 g, 0.665 mmol), NHS (0.91 g, 0.798 mmol), DCC (0.163 g, 0.798 mmol) and NEt_3 (0.11 mL, 0.798 mmol). The resultant solution was stirred for 24h at room temperature. After completion of reaction, the reaction mixture was evaporated and re-dissolved in ethyl acetate and filtered. The filtrate was washed with 0.2N H_2SO_4, saturated aq. $NaHCO_3$ and water. The organic layer was collected and dried over anhyd. Na_2SO_4 and evaporated under vacuum to obtain the crude product, which was purified by silica gel column chromatography (Ethyl acetate/Hexane in 8:2) to obtain 0.217 g of **F3** as solid.

Yield: 67%, Mp: 182 -185 ^{o}C.

^{1}H NMR (500 MHz, $CDCl_3$) δ: 0.88 (m, 30H), 0.98 (d, *J* = 6 Hz, 6H), 1.03 (d, *J* = 6.5 Hz, minor), 1.12 (br m, 2H), 1.25 (m+s, minor), 1.34 (minor),1.43 (m, 20H), 1.52 (br m, 4H), 1.78-1.96 (m, 8H), 2.00-2.10 (minor), 2.12 (br s, 2H), 2.18 (minor), 2.85 (d, *J* = 14 Hz, minor), 2.94 (d, *J* = 13.5 Hz, 2H), 3.29 (d, *J* = 13 Hz, minor), 3.40 (d, *J* = 12.5 Hz, 2H), 3.83 (d, *J* = 12.5

Hz, 2H), 3.92 (m, 2H), 4.27 (m, 2H), 4.48 (d, *J* = 13.5 Hz, 2H), 4.56 (d, *J* = 13.5 Hz, minor), 4.72 (minor), 4.88 (m, 2H), 5.13 (d, *J* = 8.0 Hz, 2H), 5.74 (d, *J* = 8.5 Hz, minor), 6.47 (d, *J* = 8.0 Hz, 2H), 6.60 (d, *J* = 7.5 Hz, 2H), 6.80 (d, *J* = 8 Hz, minor), 7.05 (br d, minor); ^{13}C NMR (100 MHz, $CDCl_3$) δ: 11.2, 15.4, 15.6 (minor), 18.0, 19.2, 19.6(minor), 21.5, 22.5 (minor), 22.8 (minor) 23.5, 24.7, 24.9, 27.5, 28.3, 29.7 (minor), 30.0 (minor), 30.4 (minor), 31.0, 36.4 (minor), 36.9, 43.1, 46.0 (minor), 46.9, 48.4 (minor), 49.8, 58.4, 59.4, 79.4 (minor), 79.7, 155.9, 170.4 (minor), 170.6, 170.8 (minor), 171.7, 171.9, 172.2 (minor); IR (KBr): 3433, 3312, 2962, 2928, 2872, 1694, 1640, 1527, 1458, 1366, 1244, 1173; HRMS calcd. for $C_{51}H_{92}N_8NaO_{10}$ m/z 999.6829, found m/z 999.6819.

Synthesis of F4

To **F3** (0.150 g, 0.153 mmol) was added ethyl acetate saturated with HCl gas (10ml) in ice cold condition. The reaction mixture was stirred for 4h at room temperature. The reaction mixture was evaporated and washed thrice with pentane to obtain 0.119 g of **F4** as white solid.

Yield: Quantitative, Mp: 200 -203 ^{o}C.

^{1}H NMR (500 MHz, CD_3OD) δ: 0.77-1.0 (m, 36H), 1.10 (m, 3H), 1.19 (m, 3H), 1.45 (m, 4H), 1.57 (m, 2H), 1.84 (m, 2H), 1.91 (m, 2H), 2.05 (m, 2H), 2.88 (d, *J* = 14.0 Hz, 2H), 3.38 (d, *J* = 12.5 Hz, 2H), 3.71 (d, *J* = 5.0 Hz, 2H), 3.81 (d, *J* = 13.0 Hz, 2H), 4.10 (d, *J* = 8.0 Hz, 2H), 4.35 (d, *J* = 13.0 Hz, 2H), 4.72 (m, 2H); ^{13}C NMR (125 MHz, CD_3OD) δ: 10.4, 13.7, 17.6, 18.3, 20.2, 22.6, 24.0, 24.5, 27.7, 29.2, 30.4, 36.9, 41.3, 46.6, 49.9, 57.3, 59.0, 167.9, 171.3, 172.2 ;IR (KBr): 3432, 3302, 2963, 2930, 1659, 1624, 1546, 1461, 1367, 1260, 1097; HRMS calcd. for $C_{41}H_{76}N_8NaO_6$ m/z 799.5780, found m/z 799.5739.

Synthesis of 1

To a well stirred and ice cooled solution of Boc-leucine (0.676 g, 2.92 mmol) in DCM was added NHS (0.336 g, 2.92 mmol), DCC (0.603 g, 2.92 mmol) followed by 1,3 diaminopropane (0.108 g, 1.46 mmol), and NEt_3 (0.4 mL, 2.92 mmol). The resultant solution was stirred for 24h at room temperature. After completion of reaction, the reaction mixture was evaporated and re-dissolved in ethyl acetate and filtered. The filtrate was washed with 0.2N H_2SO_4, saturated aq. $NaHCO_3$ and water. The organic layer was collected and dried over anhyd. Na_2SO_4 and evaporated under vacuum to obtain the crude product, which was purified by silica gel column chromatography (Ethyl acetate/Hexane in 4:6) to obtain 0.657 g of **1** as white solid.

Yield: 90%, Mp: 56 -58 ^oC.

^1H NMR (300 MHz, $CDCl_3$) δ: 0.67-1.12 (m, 12H), 1.42 (s, 18H), 1.55 (m, 2H), 1.68 (m, 6H), 3.06 (m, 2H), 3.26 (minor), 3.51 (m, 2H), 4.12 (m, 2H), 4.32 (minor), 5.14 (minor), 5.33 (m, 2H), 7.01 (minor), 7.44 (br s, 2H); ^{13}C NMR (75 MHz, $CDCl_3$) δ: 21.8, 21.9, 22.9, 24.7, 28.3, 29.7, 37.1, 40.8, 41.6, 52.0, 53.5, 79.8, 80.1, 155.7, 156.3, 174.3, 176.7; IR (KBr): 3454, 3339, 2965, 2871, 1715, 1680, 1541, 1446, 1391, 1367, 1276, 1247, 1177, 1049; HRMS calcd. for $C_{25}H_{48}N_4NaO_6$ m/z 523.3466, found m/z 523.3469.

Synthesis of F5

To a well stirred and ice cooled solution of compound **1** (0.400 g, 0.800 mmol) in DCM (10 mL) was added TFA (2.6 mL, 31.95 mmol), and the reaction mixture was stirred for 4h at room temperature. The reaction mixture was evaporated and used as such for further reaction. The obtained amine was added to the DCM solution of Boc-valine (0.347 g, 1.600 mmol), NHS (0.221 g, 1.92 mmol), DCC (0.394 g, 1.92 mmol) and NEt_3 (0.26 mL, 1.92 mmol). The resultant solution was stirred for 24h at room temperature. After completion of reaction, the

reaction mixture was evaporated and re-dissolved in ethyl acetate and filtered. The filtrate was washed with 0.2N H_2SO_4, saturated aq. $NaHCO_3$ and water. The organic layer was collected and dried over anhyd. Na_2SO_4 and evaporated under vacuum to obtain the crude product, which was purified by silica gel column chromatography (Ethyl acetate/Hexane in 8:2) to obtain 0.419 g of **F5** as white solid.

Yield: 75%, Mp: 162 -164 ^oC.

^1H NMR (300 MHz, DMSO-d_6) δ: 0.72-0.93 (m, 24H), 1.38 (s + m, 24H), 1.56 (m, 2H), 1.92 (m, 2H), 3.01 (m, 4H), 3.75 (m, 2H), 4.28 (m, 2H), 6.78 (d, J = 9 Hz, 2H), 7.76 (d, J = 8.1 Hz, 2H), 7.89 (br s, 2H); ^{13}C NMR (75 MHz, DMSO-d_6) δ: 18.7, 19.6, 22.1, 23.4, 24.5, 28.6, 29.5, 30.6, 36.7, 41.7, 51.3, 60.4, 78.5, 155.9, 171.5, 172.2; IR (KBr); 3442, 3300, 2961, 2933, 2873, 1691, 1648, 1549, 1524, 1390, 1367, 1298, 1247, 1173; HRMS calcd. for $C_{35}H_{66}N_6NaO_8$ m/z 721.4834, found m/z 721.4855.

Synthesis of 4

To a well stirred and ice cooled solution of compound **3** (998 g, 3.158 mmol) in DCM (10 mL) was added TFA (4.84 mL, 63.20 mmol), and the reaction mixture was stirred for 4h at room temperature. The reaction mixture was evaporated and used as such for further reaction. The obtained amine was added to the DCM solution of Boc-leucine (0.608 g, 2.632 mmol), NHS (0.363 g, 3.158 mmol), DCC (0.647 g, 3.158 mmol) and NEt_3 (0.44 mL, 3.158 mmol). The resultant solution was stirred for 24h at room temperature. After completion of reaction, the reaction mixture was evaporated and re-dissolved in ethyl acetate and filtered. The filtrate was washed with 0.2N H_2SO_4, saturated aq. $NaHCO_3$ and water. The organic layer was collected and dried over anhyd. Na_2SO_4 and evaporated under vacuum to obtain the crude product,

which was purified by silica gel column chromatography (Ethyl acetate/Hexane in 4:6) to obtain 0.901 g of **4** as semi-solid.

Yield: 79.7%

^{1}H NMR (500 MHz, $CDCl_3$) δ: 0.91 (d + d, *J* = 7.5 Hz,6H), 0.99 (d + d, minor) 1.34 (s, minor) 1.43 (s, 9H), 1.53 (t, *J* = 7 Hz, 2H), 1.60-1.82 (major + minor m, 3H), 1.93 (br t, 4H), 2.08 (m, minor), 2.34 (m, 2H), 2.83-3.23 (major + minor m, 4H), 3.34 (d, *J* = 12.5 Hz, minor), 3.50 (major + minor, 1H), 3.82 (d, *J* = 13 Hz, 1H), 4.02 (d, *J* = 13 Hz, minor), 4.35 (d, *J* = 13.5 Hz, 1H), 4.57 (d, *J* = 13.5 Hz, 1H), 4.65 (m, 1H), 4.80 (br m, minor), 5.48 (d, *J* = 9 Hz, 1H), 5.67 (d, *J* = 6.5 Hz, minor), 7.22 (m, 5H), 7.28 (m, minor); ^{13}C NMR (125 MHz, $CDCl_3$) δ: 21.9, 22.1, 22.7, 23.4, 23.8, 24.6, 24.7, 28.3, 28.4, 28.5, 28.9, 29.2, 29.3, 29.5, 29.7, 30.8, 31.8, 31.9, 42.7, 46.6, 48.7, 48.9, 49.4, 50.0, 57.7, 58.1, 58.8, 59.6, 63.4, 63.5, 79.0, 79.1, 126.7, 126.9, 128.2, 128.7, 137.9, 138.2, 155.5, 155.8, 171.3, 171.6; IR (KBr):3418, 2958, 2929, 2869, 1708, 1635, 1504, 1453, 1367, 1249, 1169, 1047; HRMS calcd. for $C_{25}H_{40}N_3O_3$ m/z 430.3064, found m/z 430.3071.

Synthesis of 5

To a well stirred and ice cooled solution of compound **4** (0.499 g, 1.162 mmol) in DCM (10 mL) was added TFA (1.78 mL, 23.27 mmol), and the reaction mixture was stirred for 4h at room temperature. The reaction mixture was evaporated and used as such for further reaction. The obtained amine was added to the DCM solution of Boc-Valine (0.210 g, 0.968 mmol), NHS (0.133 g, 1.162 mmol), DCC (0.238 g, 1.162 mmol) and NEt_3 (0.16 mL, 1.162 mmol). The resultant solution was stirred for 24h at room temperature. After completion of reaction, the reaction mixture was evaporated and re-dissolved in ethyl acetate and filtered. The filtrate

was washed with 0.2N H_2SO_4, saturated aq. $NaHCO_3$ and water. The organic layer was collected and dried over anhyd. Na_2SO_4 and evaporated under vacuum to obtain the crude product, which was purified by silica gel column chromatography (Ethyl acetate/Hexane in 5:5) to obtain 0.419 g of **5** as semi-solid.

Yield: 82%

^{1}H NMR (400 MHz, $CDCl_3$) δ: 0.79-0.97 (m, 12H), 0.99 (br d, minor) 1.44 (s, 9H), 1.58 (m, 2H), 1.69 (m, 4H), 1.88-2.16 (m, 5H), 2.38 (m, 1H), 2.88 (minor), 2.97 (m, 2H), 3.18 (br d, 1H), 3.47 (m, 1H), 3.54 (m, 1H), 3.83 (m, 1H), 3.90 (minor), 3.99 (br m, 1H), 4.33 (m, 1H), 4.49 (minor), 4.99 (br d, 1H), 5.10 (br d, 1H), 6.80 (m, 1H), 7.22 (m, 5H), 7.28 (minor); ^{13}C NMR (100 MHz, $CDCl_3$) δ: 17.7, 19.4, 21.8, 23.4, 23.7, 24.7, 28.3, 29.2, 30.7, 31.1, 42.7, 46.7, 47.4, 49.4, 58.0, 59.6, 60.0, 63.5, 79.7, 126.9, 128.3, 128.7, 129.0, 129.8, 137.8, 155.8, 170.6, 171.2; IR (KBr): 3431, 3305, 2961, 2928, 2869, 1716, 1626, 1520, 1455, 1367, 1247, 1170; HRMS calcd. for $C_{30}H_{49}N_4O_4$ m/z 529.3748, found m/z 529.3733.

Synthesis of F6

To a well stirred and ice cooled solution of compound **5** (0.349 g, 0.662 mmol) in DCM (10 mL) was added TFA (1.01 mL, 13.24 mmol), and the reaction mixture was stirred for 4h at room temperature. The reaction mixture was evaporated and used as such for further reaction. The obtained amine was added to the DCM solution of Boc-Isoleucine (0.127 g, 0.552 mmol), NHS (0.076 g, 0.662 mmol), DCC (0.136 g, 0.662 mmol) and NEt_3 (0.09 mL, 0.662 mmol). The resultant solution was stirred for 24h at room temperature. After completion of reaction, the reaction mixture was evaporated and re-dissolved in ethyl acetate and filtered. The filtrate was washed with 0.2N H_2SO_4, saturated aq. $NaHCO_3$ and water. The organic layer was

collected and dried over anhyd. Na_2SO_4 and evaporated under vacuum to obtain the crude product, which was purified by silica gel column chromatography (Ethyl acetate/Hexane in 6:4) to obtain 0.286 g of **F6** as semi-solid.

Yield: 81%

^{1}H NMR (500 MHz, $CDCl_3$) δ: 0.91 (m, 18H), 1.14 (m, 2H), 1.42 (m, 9H), 1.50-1.78 (m, 6H), 1.80-2.13 (m, 5H), 2.37 (m, 1H), 2.95 (m, 3H), 3.20 (m, 1H), 3.32-3.59 (m, 2H), 3.83 (m, 1H), 3.95 (m, 1H), 4.28-4.60 (m, 2H), 5.00 (m, 1H), 5.11 (minor), 5.32 (m, 1H), 6.60 (m, 1H), 7.02 (m, 1H), 7.21 (m, 5H), 7.28 (minor); ^{13}C NMR (125 MHz, $CDCl_3$) δ: 11.3, 15.4, 18.1, 19.3, 19.4, 21.9, 23.5, 23.7, 24.7, 24.9, 28.3, 29.2, 29.7, 30.7, 31.3, 37.2, 42.7, 46.8, 47.4, 47.8, 49.5, 58.1, 58.4, 59.4, 63.5, 79.6, 126.9, 128.3, 128.7, 137.8, 155.8, 170.5, 171.6; IR (KBr): 3429, 3296, 2961, 2930, 2872, 1715, 1625, 1549, 1519, 1453, 1366, 1237, 1172; HRMS calcd. for $C_{36}H_{60}N_5O_5$ m/z 642.4588, found m/z 642.4591.

Methods: -

1. **Scanning Electron Microscopy (SEM):**

A drop of the solution in methanol was put on the glass slide, which is attached on the stub by carbon tape. The solution was allowed to dry in the air and coated with 10nm of gold. All the samples were analyzed using ZEISS EVO 50 microscope.

2. **Atomic Force Microscopy (AFM):**

A drop of the solution in methanol was put on the silicon wafer and allowed to dry in the air. All the sample were analyzed using Bruker Dimension Icon atomic force microscope. Nanoscope 5.31r software was used to analyze the data.

3. **High Resolution-Transmission Electron Microscopy (HR-TEM):**

Samples for HR-TEM were prepared by dissolving the compound in methanol. A 5µl aliquot of the sample solution was placed on a 200 mesh copper grid and samples were viewed using a TECHNAI G2 (20S-TWIN) electron microscope.

4. **Circular Dichroism (CD):**

CD spectra were recorded on an AVIV model 410 spectrometer equipped with a temperature controller using a 10 mm path length cell. The samples were prepared in methanol with a concentration of 100 µM. The melting experiments were carried out between 10 and 70 °C at 226 nm wavelength. The CD data are reported as mean residue ellipticity (MRE). MRE was calculated using the equation $\theta/10 \times C \times l \times n$, where θ is the raw data in milli degree. C is the concentration in moles per litre, l is the path length of the cell in cm and n is the number of peptide bonds.

5. Dynamic Light Scattering (DLS):

Particle size was measured by using of Malvern Zetasizer, NANO ZS90 (Malvern Instruments Limited, U.K.) equipped with a 4 mW He-Ne laser operating. Compound was dissolved in methanol and measurements were carried out in a glass cell at 25 °C.

Table S1. *J* –Coupling values of foldamers **F1**, **F2**, **F3** in $CDCl_3$.[1]

Compound	$^3J_{NH\text{-}\alpha CH}$	$^3J_{NH\text{-}\alpha CH}$	$^3J_{NH\text{-}\alpha CH}$
F1	*anti* Leu = 9 Hz *syn* Leu = 7.8 Hz		
F2	Leu = 8 Hz	*anti* Val = 9 Hz *syn* Val = 9 Hz	
F3	*anti* Leu = 7.5 Hz	*anti* Val = 8.0 Hz *syn* Val = 8.0 Hz	*anti* Ile = 8.0 Hz *syn* Ile = 8.5 Hz

Table S2. Chemical shift deviation (CSD) of C_α-protons of compounds **F2**, **F3**, **F4**, **F5**, **F6**, **1**, **4**, **5** along with literature data of random coil.[2]

Compound	Proton	δ (obs) in ppm	δ (random coil)[2] in ppm	Chemical shift deviation i.e. Δδ(CHα) = δ(CHα) (obs) - δ(CHα) (random coil) in ppm
F2	Leu (CHα) Val (CHα)	4.90 3.90	4.17 3.95	0.73 -0.05
F3	Leu (CHα) Val (CHα) Ile (CHα)	4.88 4.27 3.92	4.17 3.95 3.95	0.71 0.32 -0.03
F4	Leu (CHα) Val (CHα) Ile (CHα)	4.72 4.10 3.71	4.17 3.95 3.95	0.55 0.15 -0.24
F5	Leu (CHα) Val (CHα)	4.28 3.75	4.17 3.95	0.11 -0.20
F6	Leu (CHα) Val (CHα) Ile (CHα)	5.00 4.38 3.95	4.17 3.95 3.95	0.83 0.43 0
1	Leu (CHα)	4.12	4.17	-0.05
4	Leu (CHα)	4.80	4.17	0.63
5	Leu (CHα) Val (CHα)	4.99 3.99	4.17 3.95	0.82 0.04

Table S3. Chemical shift deviation of **F2** and **F6** compared with **F5.**

Compound	Type of proton	δ (obs) in ppm	δ (**F5**) in ppm	Chemical shift deviation i.e. Δδ(CHα) = δ(CHα) (obs) - δ(CHα) (**F5**) in ppm
F2	Leu (CHα) Val (CHα)	4.90 3.90	4.28 3.75	0.62 0.15
F6	Leu (CHα) Val (CHα)	4.99 3.99	4.28 3.75	0.71 0.24

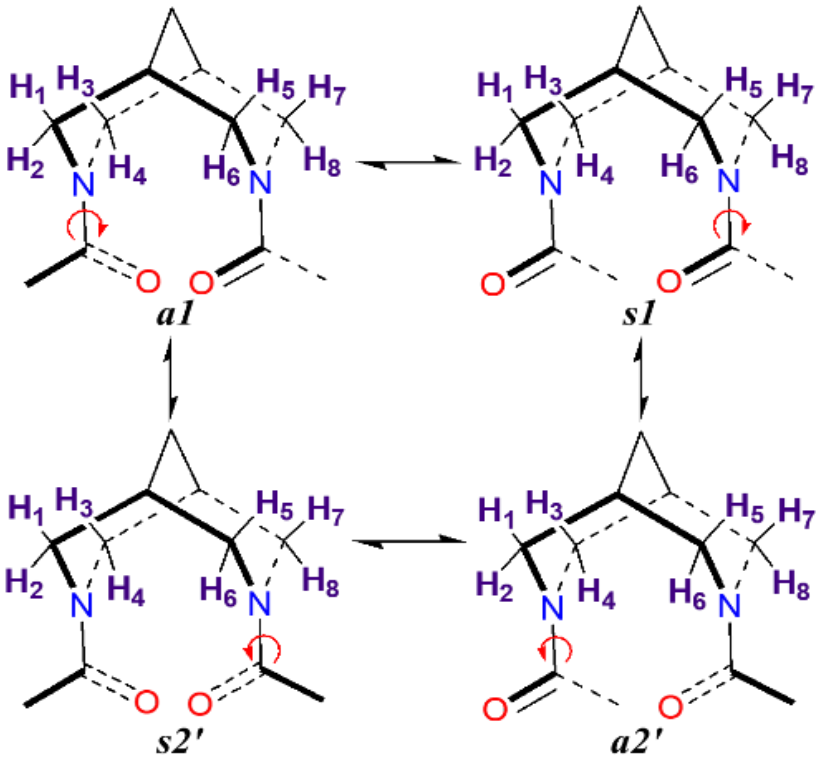

Fig. S1. The conformations of bispidine diamides. The equatorial hydrogen atoms that are proximal to the carbonyl oxygen atoms are labelled. There are two *anti* (*a1* and *a2'*) and two *syn* (*s1* and *s2'*) forms.

Dynamic NMR experiments

Selective and non-selective inversion recovery experiments were performed on the interested sites with varying mixing delay at each temperature. The axial hydrogen $H_{1,7}$ signal was inverted using a selective pulse which was calibrated using "paropt" command. The integrated peak area was fitted using MATLAB R2020a for non-selective experiments and using the CIFIT program (specifically designed for exchange data fitting) for selective experiments.

The fitted data is shown in **Fig. S2a**. The dotted line shows the inverted peak (*anti*-conformer) and solid line (*syn*-conformer) is the exchanging counter part of the former peak (Normalized intensity). The exchange effect can be seen on the minor exchange peak in initial part of the time.

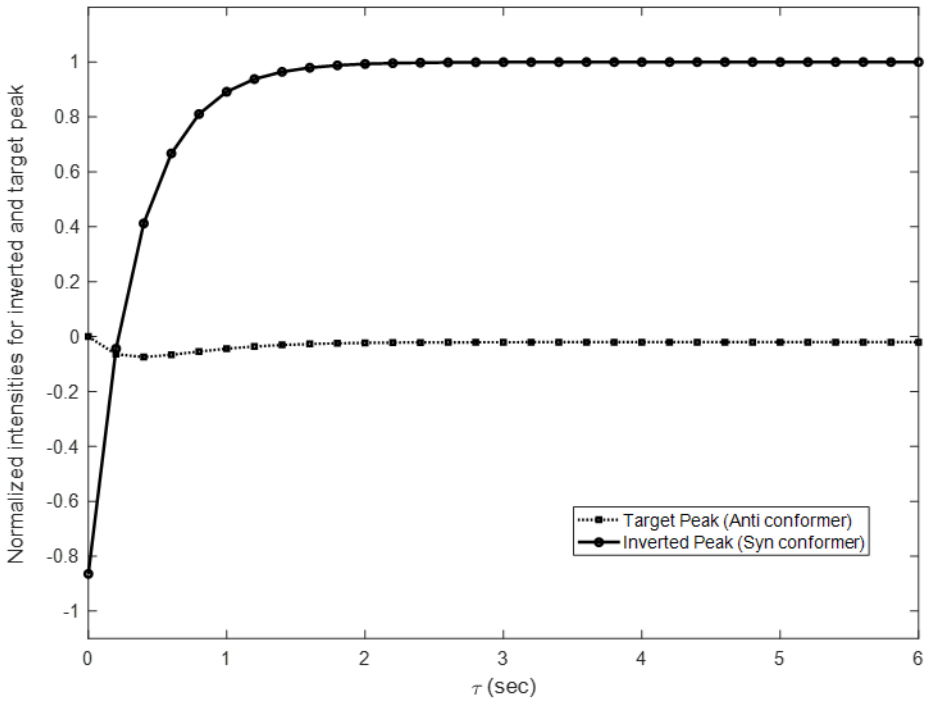

Fig. S2a. Plot of normalized intensities of the inverted peak (solid line) and target peak (dotted line) against the mixing delay varied at 25°C.

These profiles are fitted for these peaks at several temperatures to get the exchange rate (k). The summarized data is given below in **Table S4**. The temperature range is 278K-303K.

The $\ln(k)$ vs. $1/T$ (Arrhenius plot) gives the activation energy $\Delta E^{\ddagger}$

$$k = A \exp\left(-\frac{\Delta E^{\ddagger}}{RT}\right)$$

where *A* is the pre-exponential factor, *R* is the gas constant. (**Fig. S2b**)

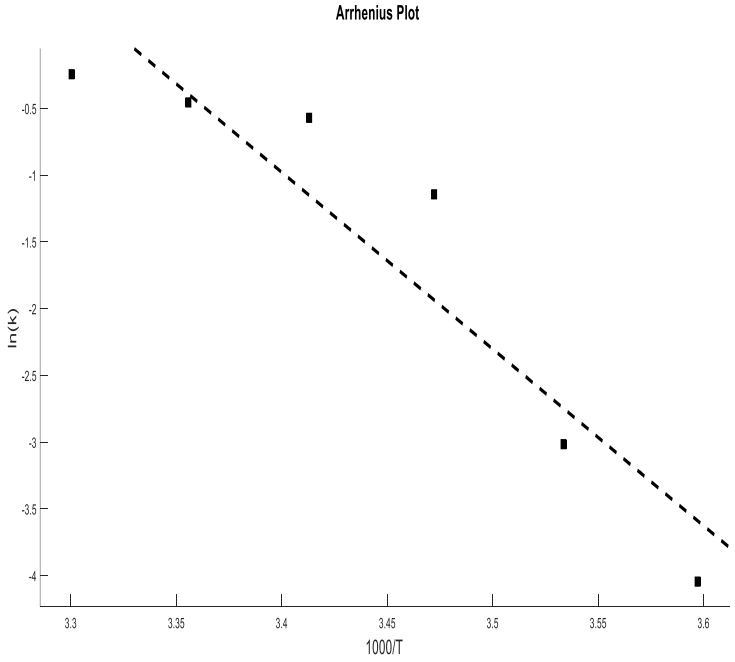

Fig. S2b: Plot of $\ln(k)$ against $1000/T$. Calculating the value of slope from the fitted equation (dotted line), the activation energy was obtained (mentioned in **Table S5**).

Table S4: Exchange rate data at different temperatures.

T(K)	1/T1 of peak at 3.05 ppm (s^{-1})	1/T1 of peak at 2.87 ppm (s^{-1})	k (s^{-1})
278	2.76	3.25	0.02
283	2.82	3.34	0.05
288	2.95	3.52	0.32
293	3.01	3.61	0.57
298	3.07	3.71	0.63
303	3.14	3.82	0.78

Also, Eyring plot gives the enthalpy of activation and entropy:

$$k = \frac{k_B T}{h} \exp\left(-\frac{\Delta G^{\ddagger}}{RT}\right)$$

$$k = \frac{k_B T}{h} \exp\left(\frac{\Delta S^{\ddagger}}{R} - \frac{\Delta H^{\ddagger}}{RT}\right)$$

where, k_B is the Boltzmann's constant, h is Planck's constant, $\Delta G^{\ddagger}$ is the free energy of activation, $\Delta S^{\ddagger}$ is the entropy of activation and $\Delta H^{\ddagger}$ is the enthalpy of activation. The fit is shown in **Fig. S2c**.

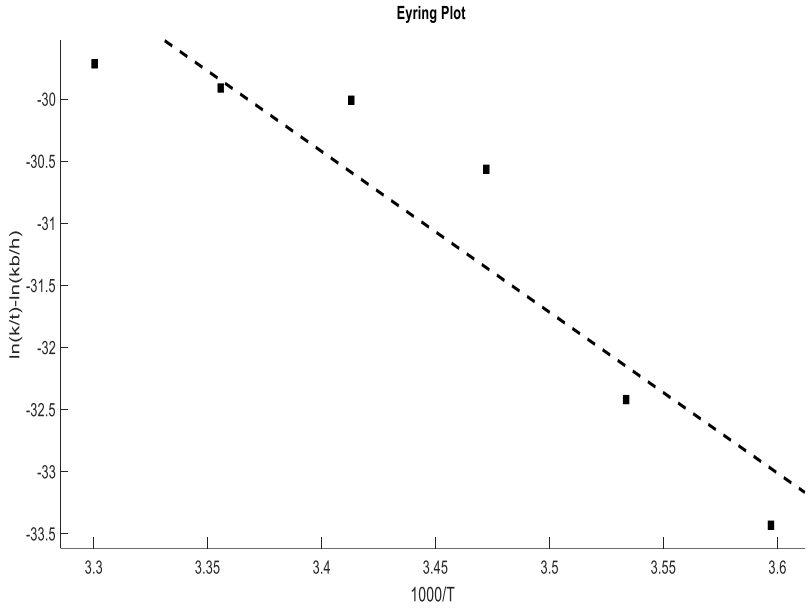

Fig. S2c: Plot of (ln(k/t)-ln(k_b/h) against $1000/T$. Calculating the slopes and intercept from the fitted equation the values of Enthalpy of activation and Entropy of activation were obtained (mentioned in **table S5**).

Table S5: Activation energy barrier ($\Delta E^{\ddagger}$) and the standard enthalpy of activation ($\Delta H^{\ddagger}$) and entropy based on NMR experiments.

$\Delta E^{\ddagger}$ (kJ/mole)	$\Delta H^{\ddagger}$(kJ/mole)	$\Delta S^{\ddagger}$(J/K/mole)
110 ± 14	108 ± 13	118 ± 47

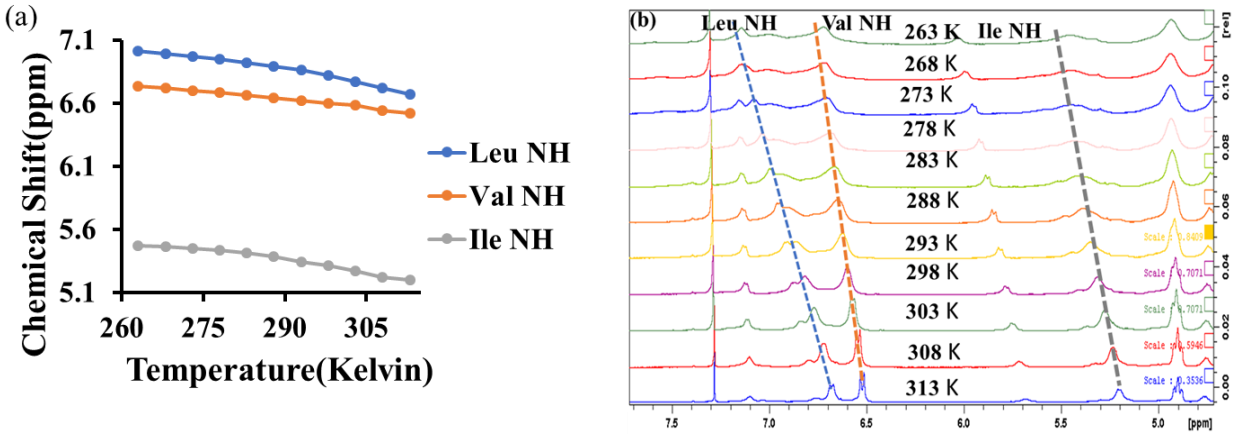

Fig. S3. (a) Plot of temperature dependence of NHs chemical shifts of **F3** in $CDCl_3$ (500 MHz) solution (b) ^1H NMR spectrum of **F3** in $CDCl_3$ (500 MHz) solvent at different temperature showing the change in chemical shift of amide NHs with temperature.

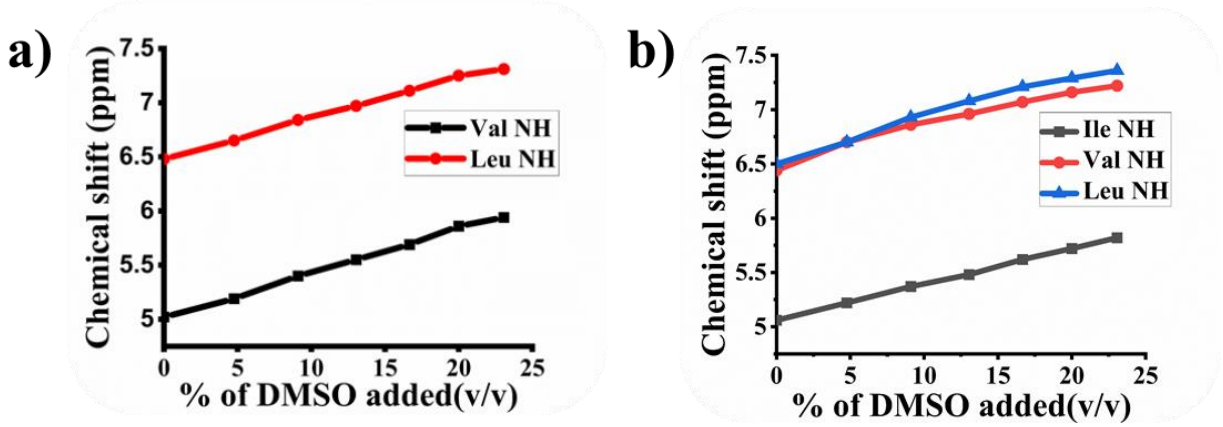

Fig. S4 (a) and (b) showing chemical shift δ_{NH} of amide protons of **F2** and **F3** in $CDCl_3$ (500 MHz) upon increasing amount of DMSO-d_6 respectively.

Table S6. Crystal data and structure refinement for **F1** (CCDC 2099286).

Identification code	shelx	
Empirical formula	C29 H52 N4 O6	
Formula weight	522.746	
Temperature	293(2) K	
Wavelength	0.71073Å	
Crystal system	Monoclinic	
Space group	P 1 21 1	
Unit cell dimensions	a = 11.5887(4) Å	α= 90°.
	b = 12.1505(4) Å	β= 97.342(3)º.
	c = 14.5684(6) Å	γ = 90°.
Volume	2034.54(13) $Å^3$	
Z	2	
Density (calculated)	1.292 Mg/m^3	
Absorption coefficient	0.465 mm^{-1}	
F(000)	836	
Crystal size	0.21 x 0.11 x 0.22 mm^3	
Theta range for data collection	3.281 to 27.424°.	
Index ranges	-14<=h<=14, -15<=k<=1, -18<=l<=18	
Reflections collected	29308	
Independent reflections	8248 [R(int) = 0.0477]	
Completeness to theta = 24.998°	100.0 %	
Refinement method	Full-matrix least-squares on F3	
Data / restraints / parameters	8248 / 1 / 461	
Goodness-of-fit on F3	0.953	
Final R indices [I>2sigma(I)]	R1 = 0.0775, wR2 = 0.2101	
R indices (all data)	R1 = 0.1163, wR2 = 0.2428	
Absolute structure parameter	0.05(3)	
Extinction coefficient	n/a	
Largest diff. peak and hole	0.265 and -0.599 $e.Å^{-3}$	

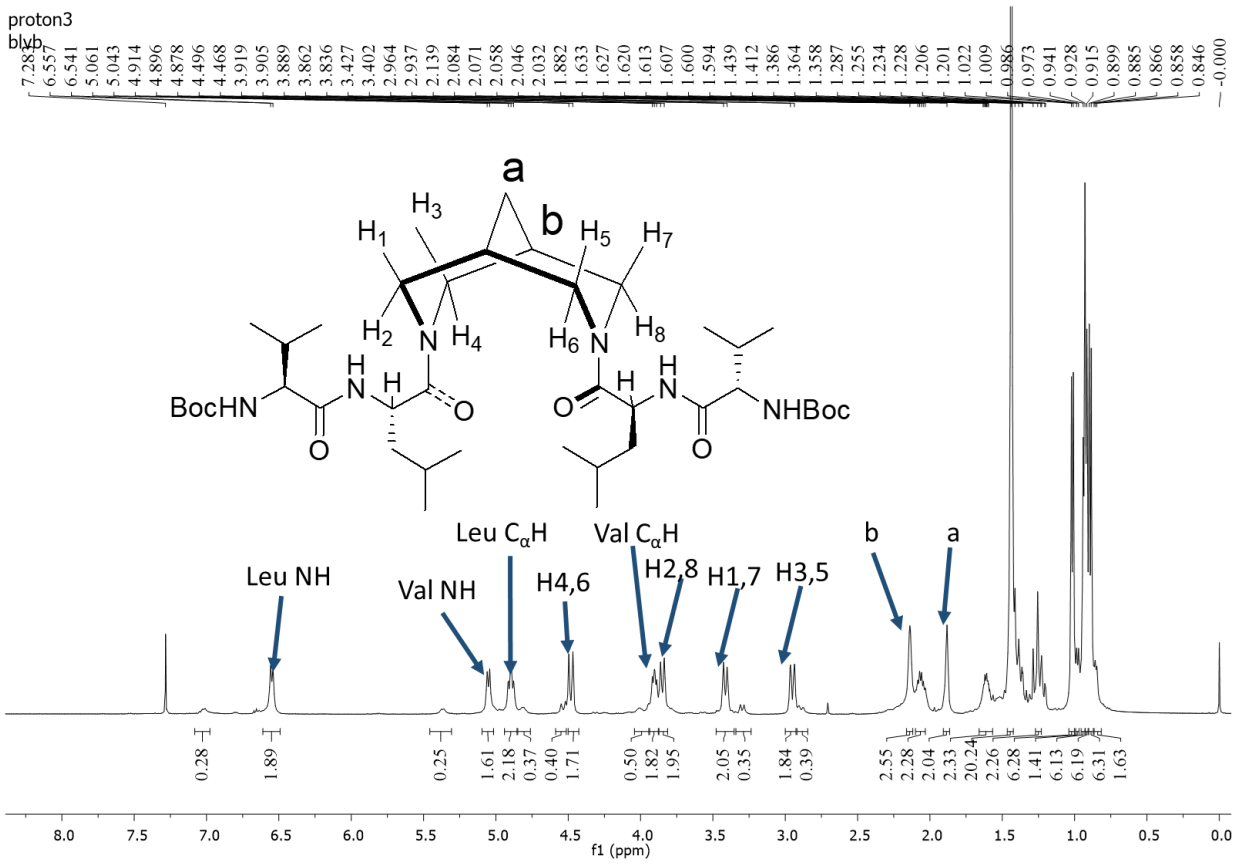

Fig. S5a. ^{1}H NMR ($CDCl_3$, 500 MHz) of **F2** indicating the signals corresponding to *anti*-form**.**

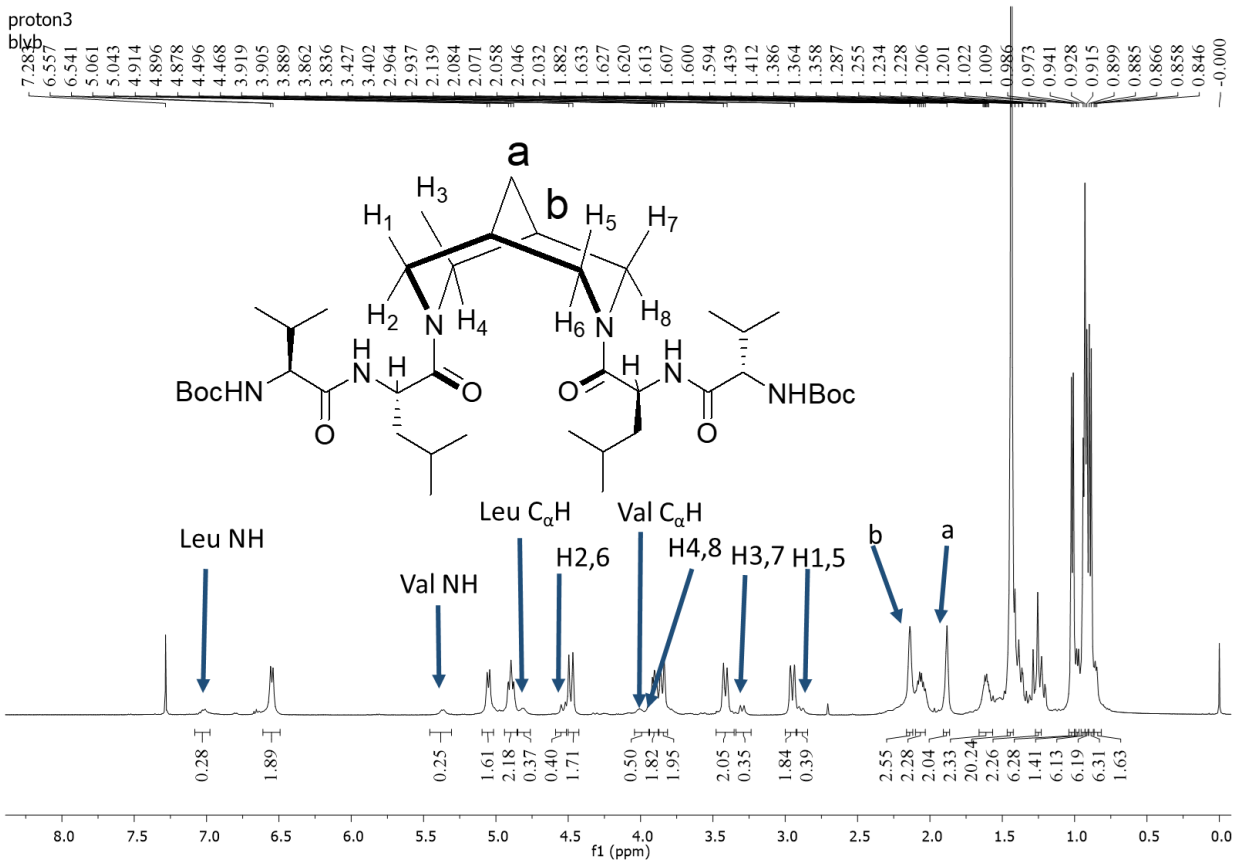

Fig. S5b. ^{1}H NMR ($CDCl_3$, 500 MHz) of **F2** indicating the signals corresponding to *syn* form**.**

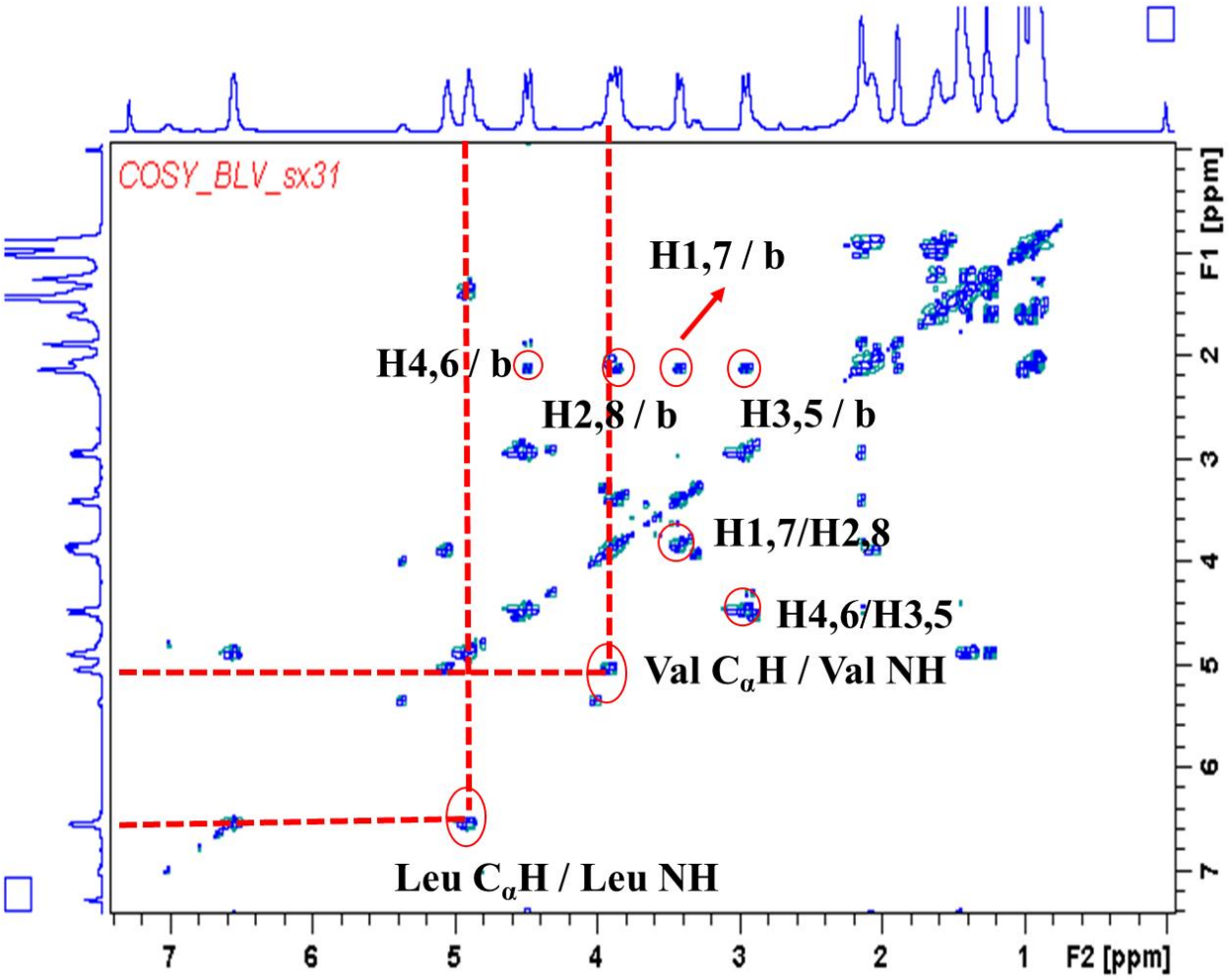

Fig. S5c. COSY spectrum of **F2** ($CDCl_3$, 400 MHz).

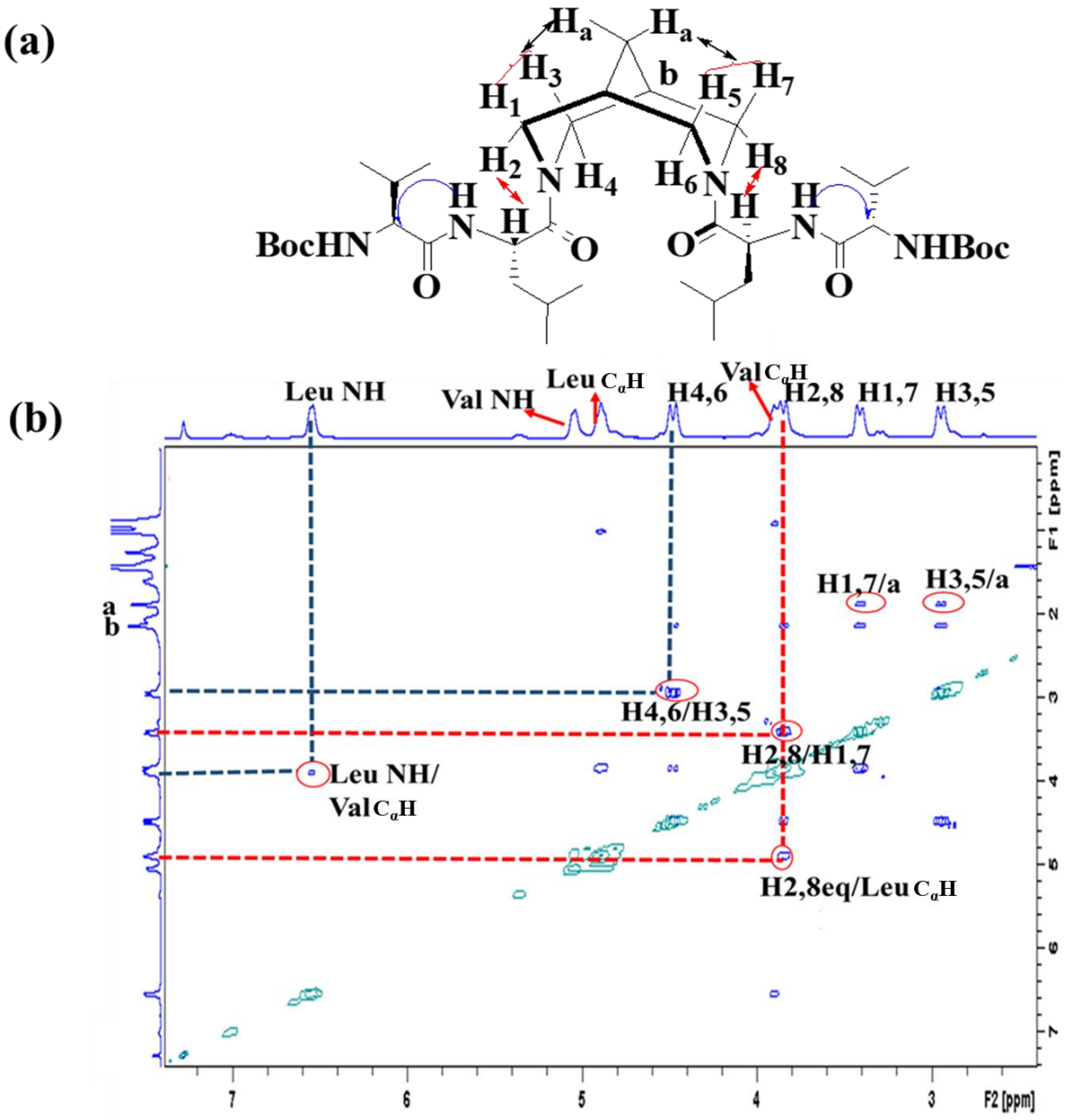

Fig. S5d. Partial ROESY spectrum of **F2** ($CDCl_3$, 400 MHz) showing correlations of Leu $C_\alpha H$ with bispidine equatorial H.

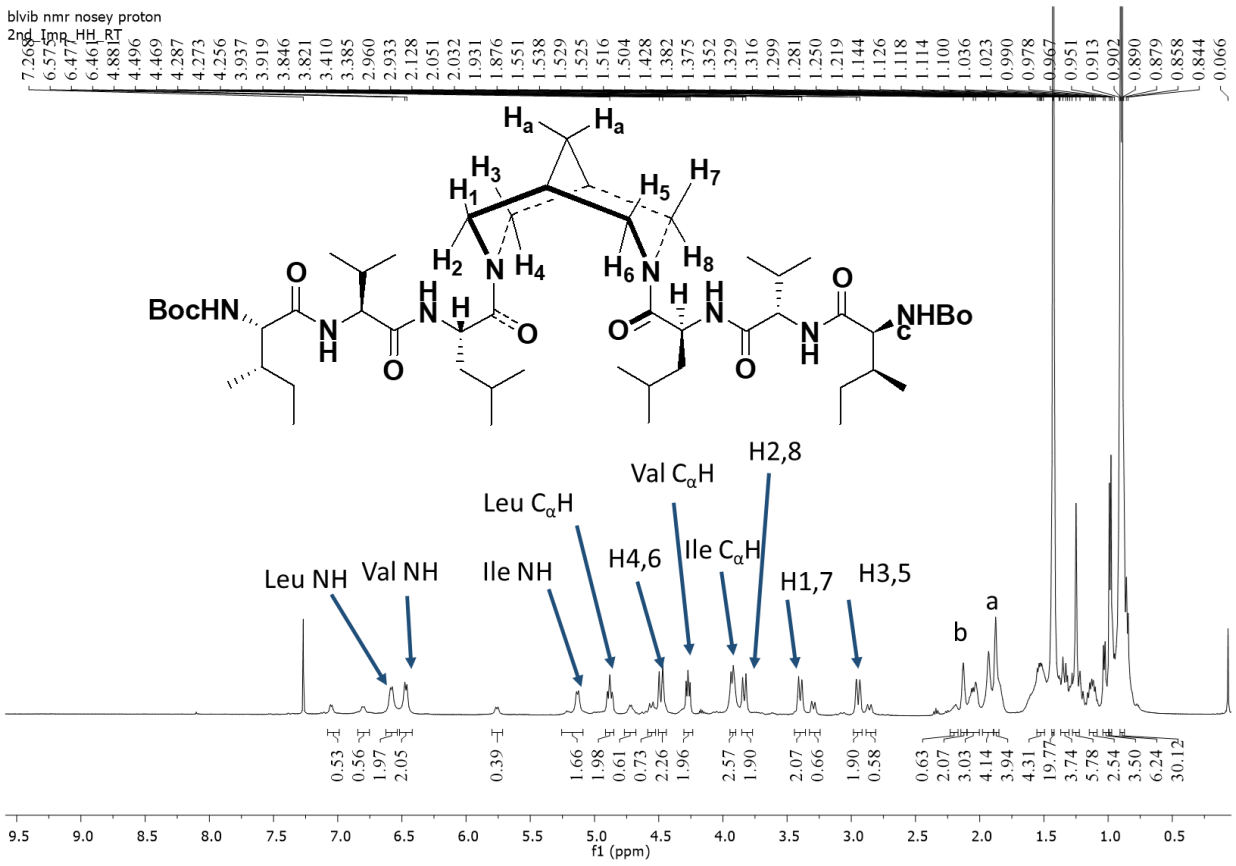

Fig. S5e. ^{1}H NMR ($CDCl_3$, 500 MHz) of **F3** indicating the signals corresponding to *anti*-form**.**

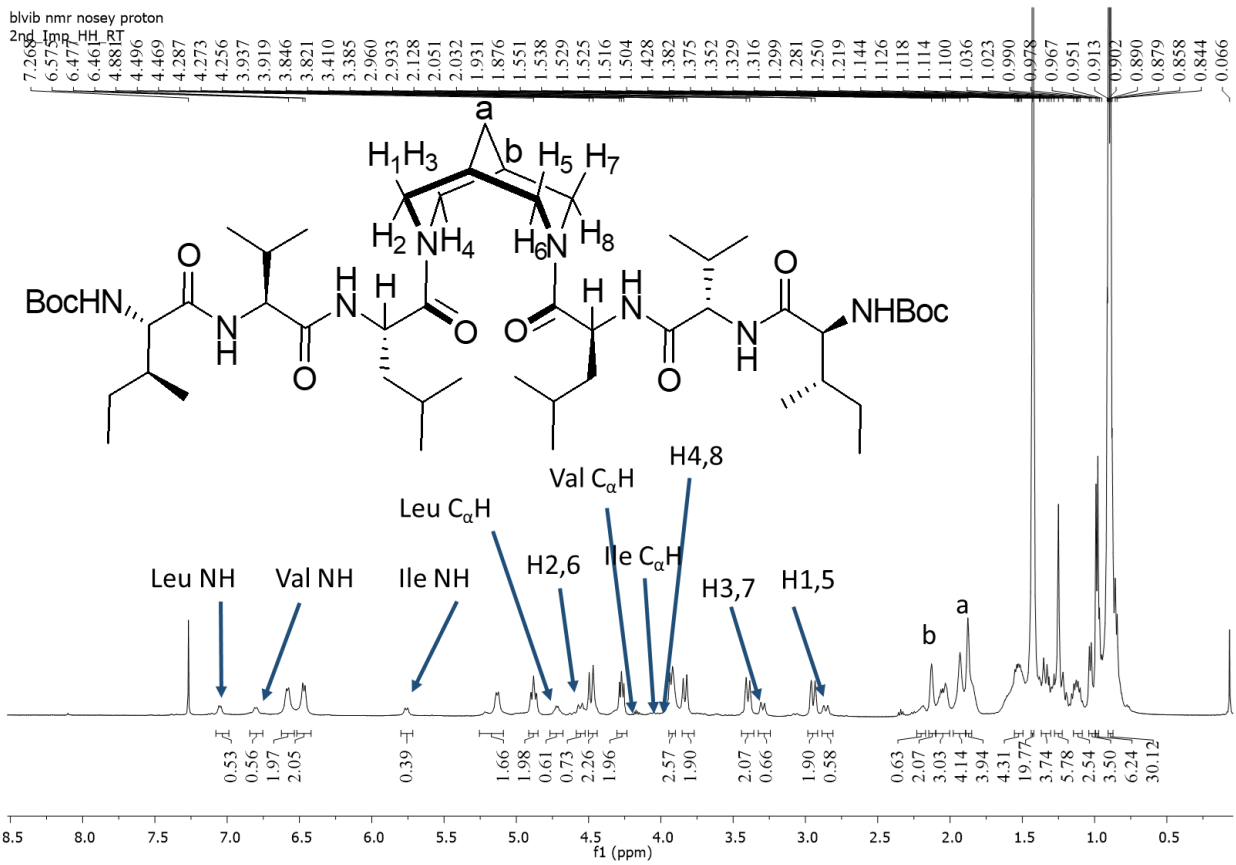

Fig. S5f. ^{1}H NMR ($CDCl_3$, 500 MHz) of **F3** indicating the signals corresponding to *syn* form**.**

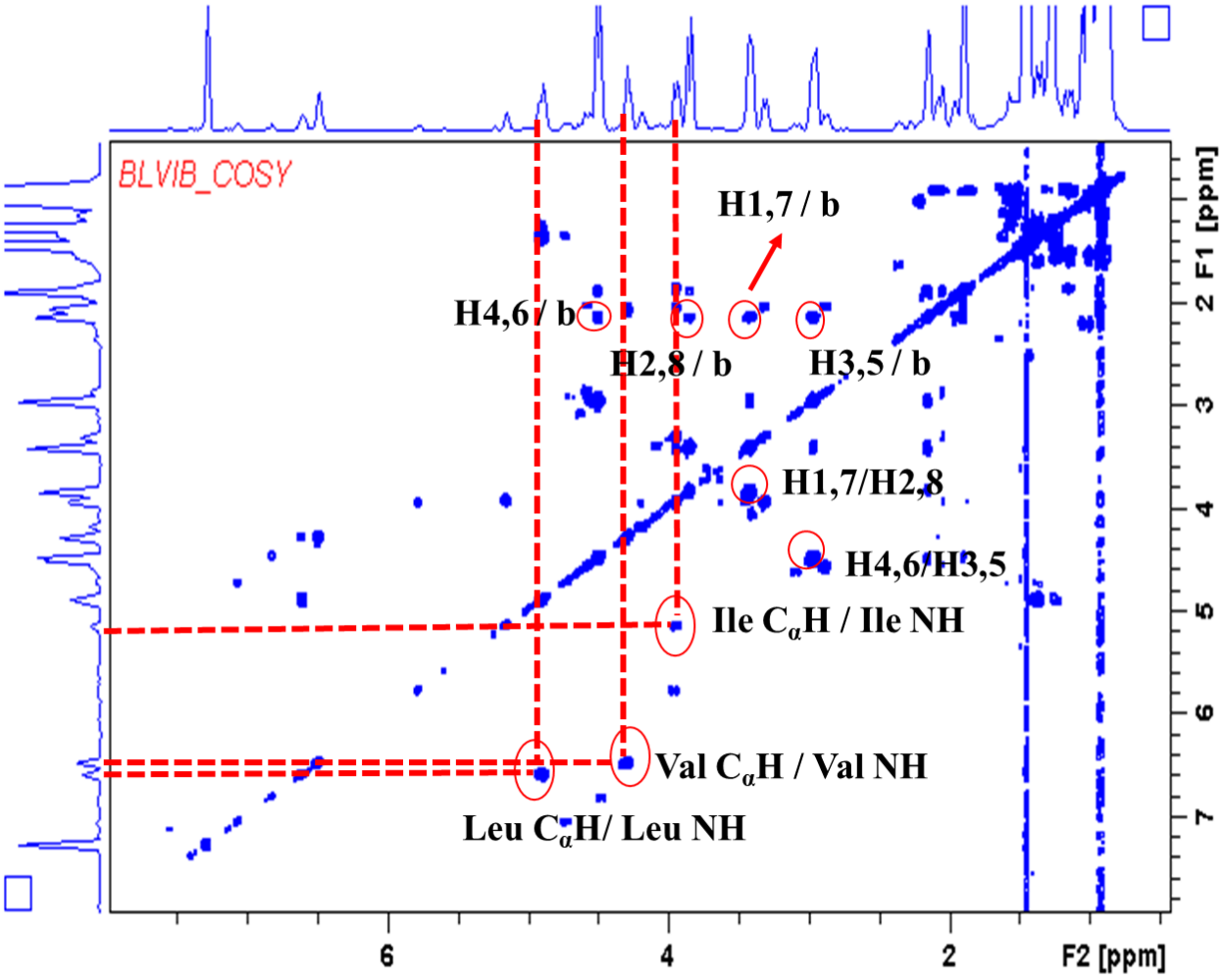

Fig. S5g. COSY spectrum of **F3** ($CDCl_3$, 500 MHz).

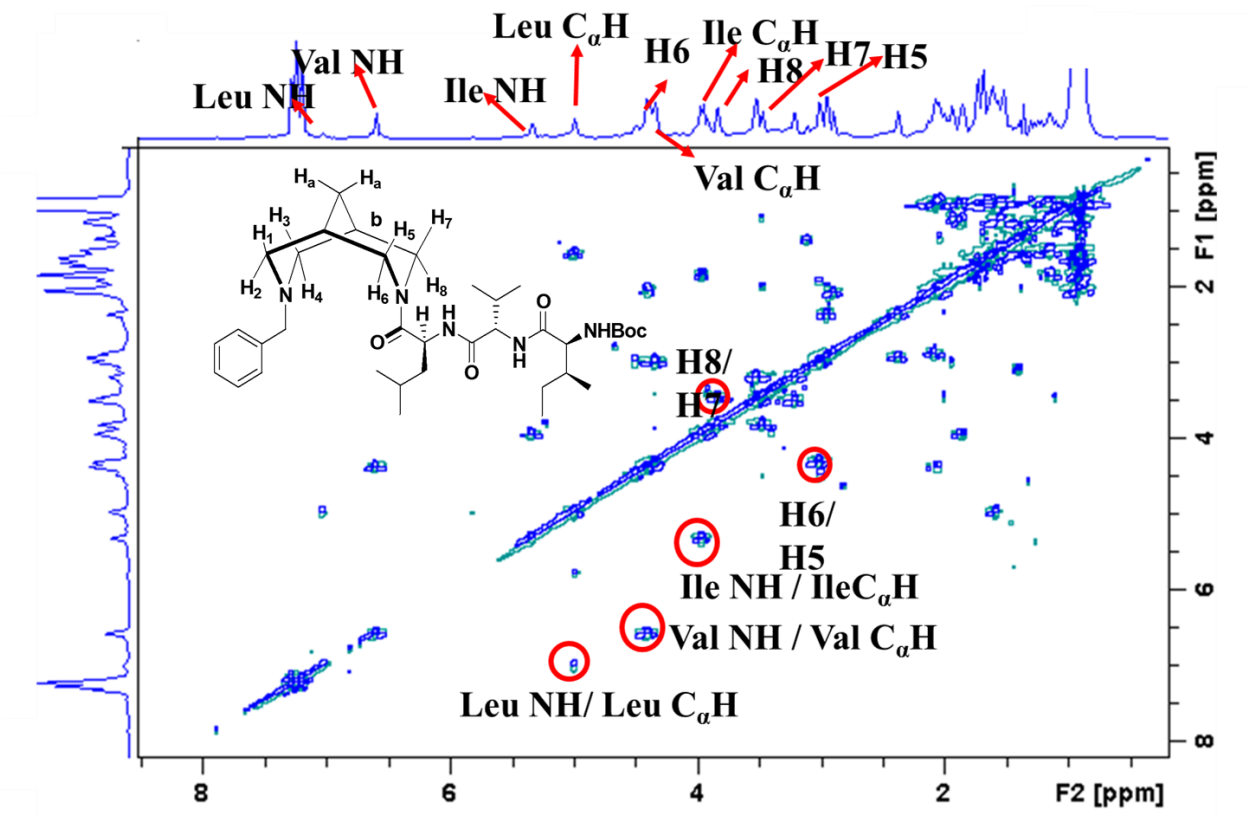

Fig. S5h. COSY spectrum of **F6** ($CDCl_3$, 400 MHz).

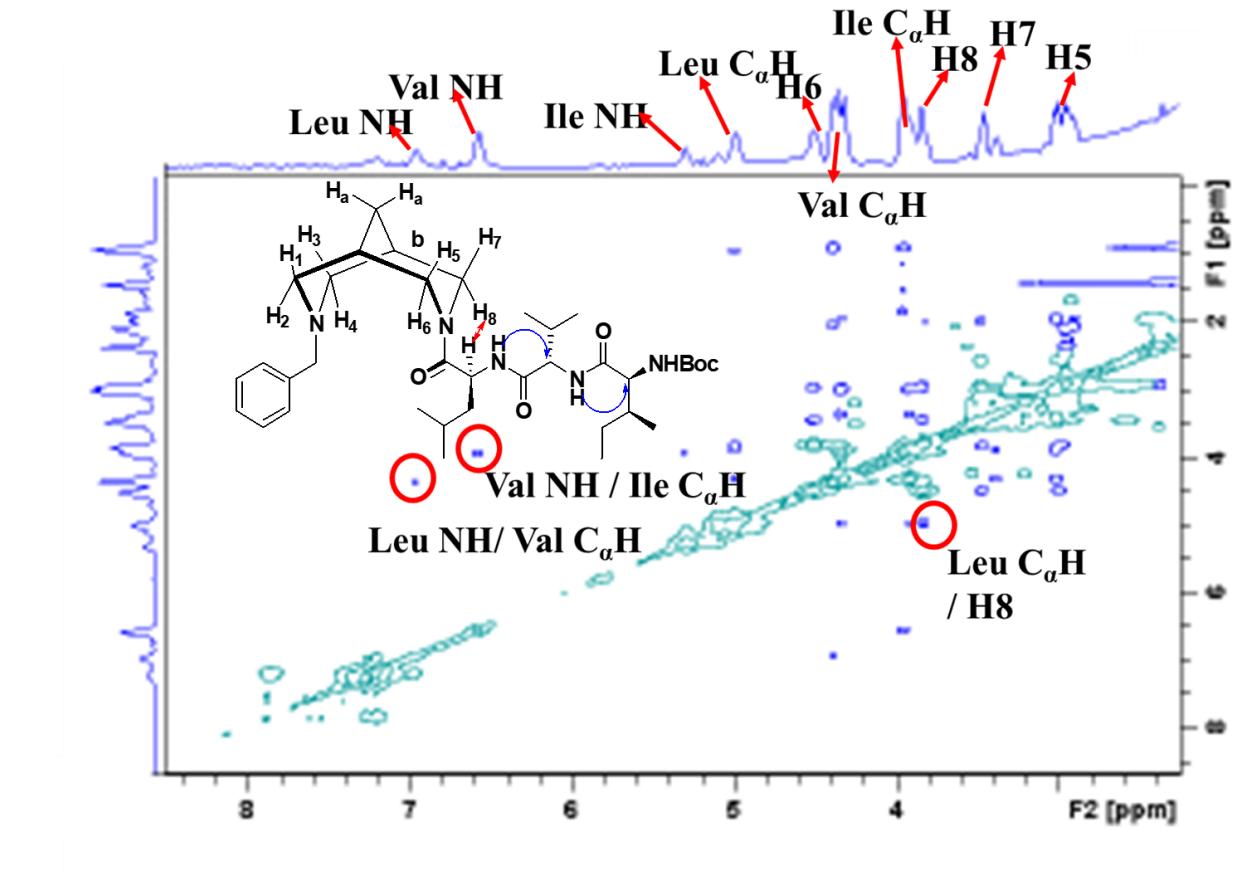

Fig. S5i. Partial ROESY spectrum of **F6** ($CDCl_3$, 400 MHz) showing correlations of Leu C_αH with bispidine equatorial H.

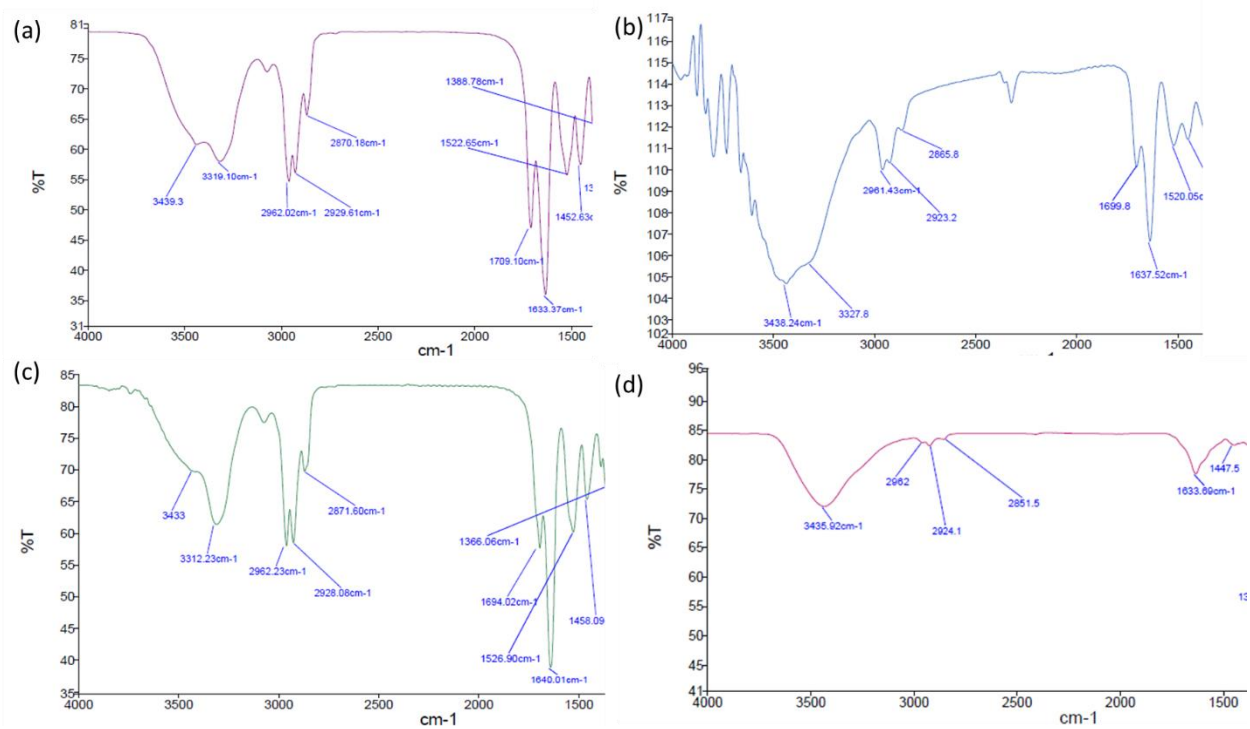

Fig. S6. (a & c) are IR (KBr) of **F2** and **F3** respectively. (b & d) are IR spectra in chloroform solution of **F2** and **F3** respectively.

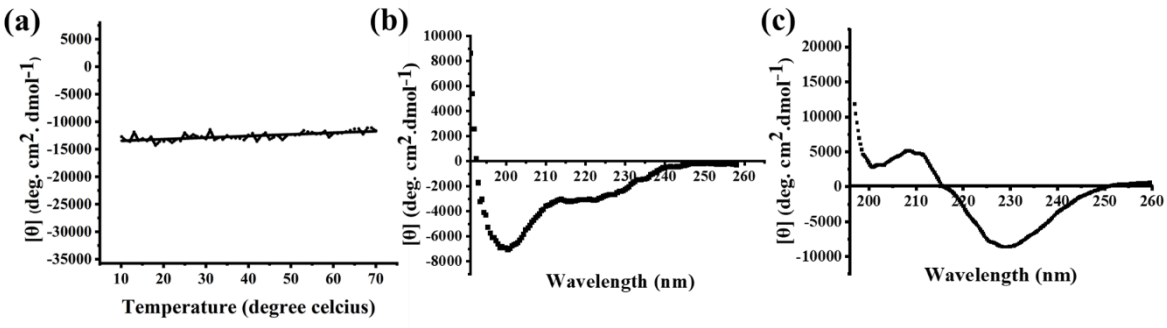

Fig. S7. (a) Temperature dependent CD data of **F3** measured at wavelength 226 nm. (b) CD spectrum of compound **F6**. **(c)** CD spectrum of compound **F5**.

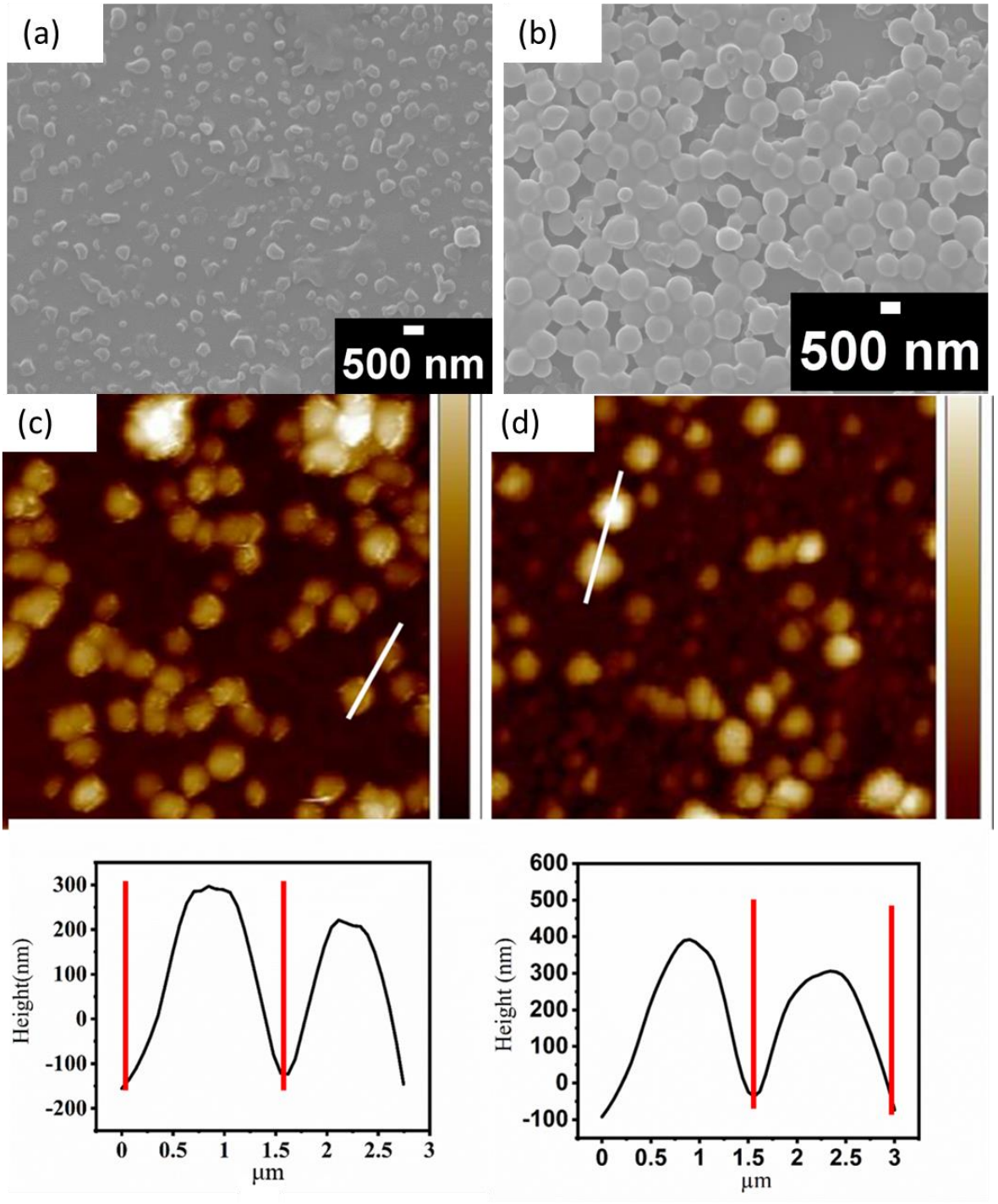

Fig. S8. (a) and (b) are the SEM images of **F5** and **F3** at 0.5 mg/ml in methanol. (c) AFM image of **F2** at 0.25 mg/ml and (d) AFM image of **F2** at 0.5 mg/ml. Below is the corresponding height profile of the highlighted part.

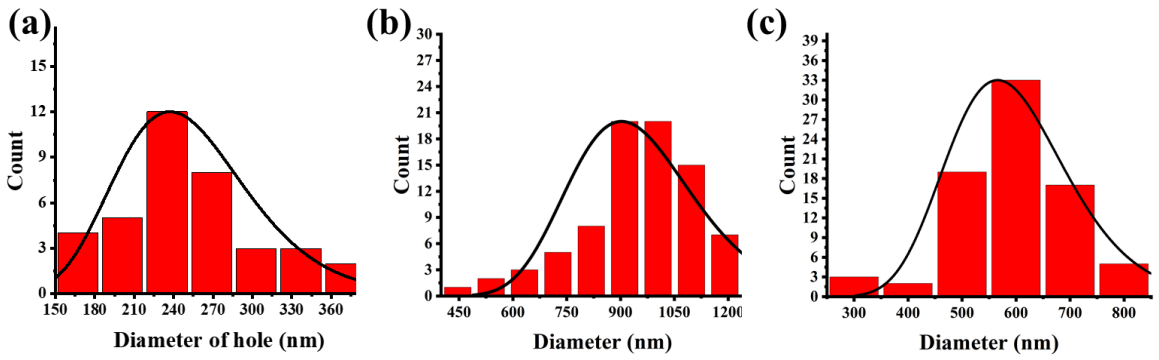

Fig. S9. Histogram based on SEM images (a) Size distributions of diameters of hollow cages at 0.25 mg/ml of **F2** (b) Size distributions in diameters of vesicles at 0.5 mg/ml of **F2** (c) Size distribution of diameters of vesicles at 0.5 mg/ml of **F3**.

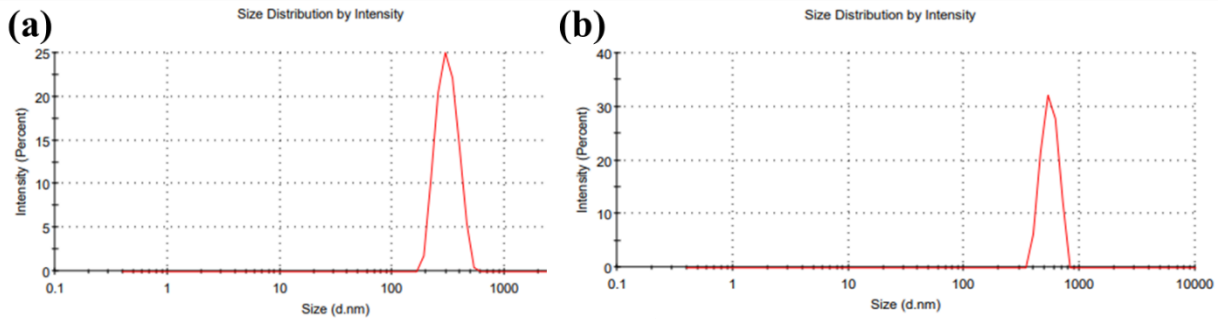

Fig. S10. Dynamic light scattering (DLS) profiles of **F2** (a) **F2** at 0.25 mg/ml in methanol (b) **F2** at 0.5 mg/ml in methanol.

2. Supplementary Data from Computational Modelling

2.1 Generation of starting structure of molecules for MD simulations

2.1.1 Bispidine conjugated with tripeptides (F3)

The initial structure of the bispidine linker and the attached leucine residues in *anti*-form was taken from the crystal structure of compound **F1.** The subsequent valine and isoleucine residues were connected to leucine using the "Protein Builder" tool in PyMol.[3] The N-terminal of isoleucine was capped by a Boc protecting group using "Chemical Builder" tool. The same procedure was followed in building both the arms linked to bispidine in **F3**. The final structure was auto-sculpted to remove steric clashes.

2.1.2 Bispidine placed at the C-terminus of the tripeptide (F6)

PDB file was created by using 3D chemdraw and was used for further simulation study.

2.1.3 Diaminopropane conjugated with tripeptides (F7)

The "Protein Builder" tool in Pymol was used to generate Ile-Val-Leu tripeptide in a β-strand conformation. This tripeptide was capped with a Boc-protecting group and further the 1,3-diaminopropane linker was connected to the peptide using the "Chemical Builder" tool in PyMol.

2.2 Simulation details

2.2.1 Generation of topology

The starting structures in *mol2* format were used as inputs to CGENFF to generate the topology parameters for the molecules. The output files were converted to GROMACS topology file formats (itp, prm) from the command line using *cgenff_charmm2gmx.py* script. The forcefield parameters in the generated topologies with pre-existing entries in ffnonbonded.itp and ffbonded.itp in

CHARMM36FF folder were removed. Topology parameters used for **F3**, **F7** and $CHCl_3$ are available at https://github.com/akshay-chenna/bispidine.git

2.2.2 Setup of simulation box

All-atomistic simulations of **F3, F6** and **F7** in $CHCl_3$ solvent were performed on GROMACS 2019.4[5] using CHARMM36 forcefield.[6] The total production run for **F3** was 200 ns whereas **F6** and **F7** were simulated for 100 ns. Several steps of equilibration were performed prior to generation of production trajectories. The starting structures were placed in a cubic box with size such that the minimum distance between any atom and box walls was 2 nm (*gmx editconf -d 2)*. The topology and GRO files of $CHCl_3$ were generated from SWISS-PARAM[7] (using CHARMM22 FF). *gmx insert* command was used to solvate the molecules with an appropriate number of $CHCl_3$ solvent molecules. The number of solvent molecules to be added were determined based on the empty volume in the box containing the solute as obtained from *gmx sasa -tv* while assuming a $CHCl_3$ density of 1478 g/l. We added 1850, 1300 and 2450 $CHCl_3$ molecules to solvate **F3**, **F6** and **F7** respectively.

2.2.3 Simulation protocols

The simulation box was energy-minimized (EM) using the steepest-descent algorithm until the maximum forces on atoms are under 1000 kJ/mol. To generate the correct velocities, we performed simulated annealing (SA) for 500 ps by raising the temperature of the system from 10K to 298 K. This was followed by equilibration under the canonical ensemble (NVT) at 298 K for 500 ps. Berendsen thermostat was used in SA and NVT steps with separate coupling constants for solute (τ_T = 2 ps) and solvent (τ_T = 0.5 ps). Position restraints on the backbone and linker heavy atoms (force constant k=1000 kJ/mol nm^2) were applied during the EM, SA and NVT steps. The final

equilibration step under the isobaric-isothermal ensemble (NPT) was performed for 1 ns without position restraints using the Berendsen thermostat (solute τ_T = 2 ps, solvent τ_T = 0.5 ps) and barostat (τ_P = 4 ps). The production run was performed in the NPT ensemble using the Nosè-Hoover thermostat (solute τ_T = 2 ps, solvent τ_T = 0.5 ps) and Parrinello-Rahman barostat (τ_P = 4 ps). In all equilibration and production runs, short range electrostatics were treated with Verlet cutoff-schemes with a cutoff radius of 1.2 nm for coulombic (and van der Wall's interactions). Long range electrostatics were treated with Particle Mesh Ewald (PME) method. Periodic boundary conditions were applied in the x, y, and z directions. The final trajectories were corrected for periodic boundary conditions using *whole* and *nojump* features of *gmx trjconv*.

2.2.4 Convergence of MD trajectories

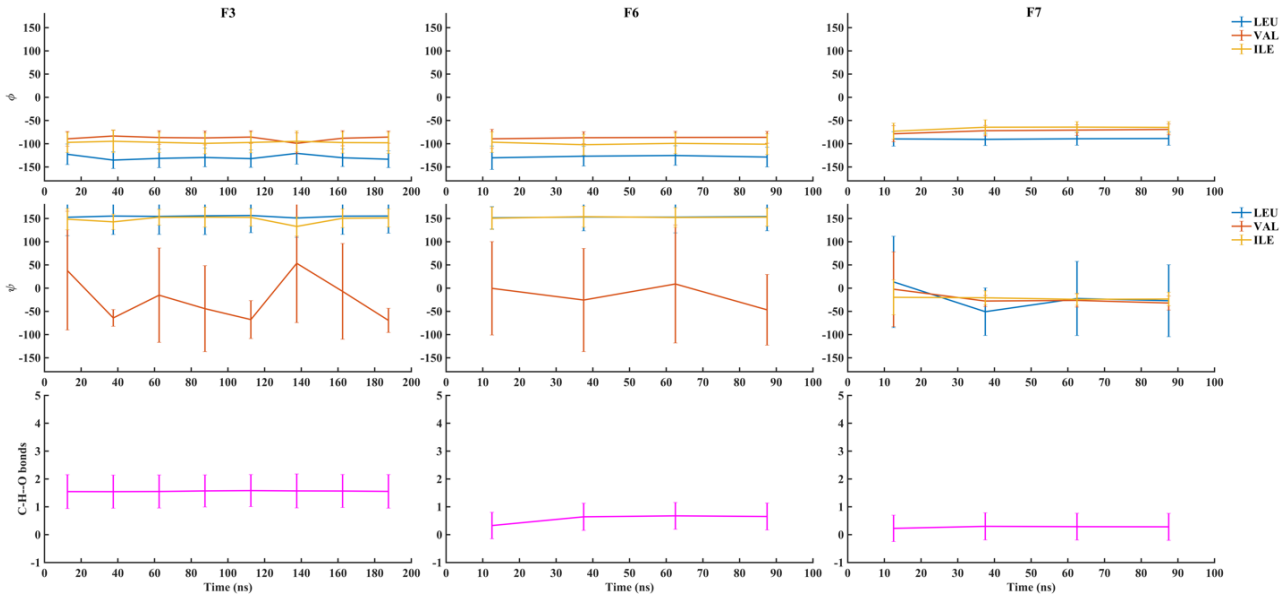

Fig. S11: Block averages calculated from 25 ns intervals of the MD trajectory are plotted for φ, ψ dihedrals and number of C-H---O bonds for single simulations of **F3**, **F6** and **F7**. The error bars reflect one standard deviation from the mean.

2.3 Analysis and comparison of properties from simulations

2.3.1 Computationally derived $^{3}J^{HNH\alpha}$ values

Table S7: $^{3}J^{HNH\alpha}$ values for Leu, Val and Ile residues present in **F3**, **F6** and **F7** are shown. Karplus equation was used to calculate the J-coupling between the H attached to backbone Nitrogen and H attached to C-alpha carbon of a particular residue. The φ-dihedrals are calculated using the default parameters of *gmx chi*[5]: A=6.51, B=-1.76, C=1.6. Values of **F3** closely resemble the experimentally determined values. Experimentally determined values are listed in **Table S1**.

	F3 $^3J^{HNH\alpha}$ (Hz)	F6 $^3J^{HNH\alpha}$ (Hz)	F7 $^3J^{HNH\alpha}$ (Hz)	F3 (in methanol) $^3J^{HNH\alpha}$ (Hz)
Leu	9.6	9.7	7.8	9.4
Val	7.7	7.8	5.7	8.7
Ile	8.1	9	5.1	7.1

2.3.2 Population of ensemble in β region of the Ramachandran plot

Table S8: The fraction of population of the total trajectory binned in the β region (φ: {−170°, −40°} and ψ: {90°, 180°}) of the Ramachandran plot is compared for **F3**, **F6** and **F7**. The φ, ψ dihedral angles for each residue were plotted (Ramachandran plots) and the fractions were obtained using the *rama* function in Bioinformatics Toolbox of MATLAB2020b. **Table S8** supports **Tables S1** and **S7** by quantifying the propensity for the molecules to adopt a β strand conformation.

	F3	F6	F7	F3 (in methanol)	Acetyl capped F3 (in water)
Leu	98 %	98 %	14 %	87 %	96 %
Val	30 %	25 %	8 %	62 %	92 %
Ile	60 %	98 %	6 %	30 %	48 %

2.3.3 Cluster analysis of MD trajectories

Table S9: The most populated clusters as obtained from simulations. *gmx cluster* command line tool was used to cluster the trajectories after periodic boundary corrections. *Gromos* method was

applied to cluster on the basis of backbone atoms of the residues and heavy atoms of the linker. A cutoff of 0.1 nm was used to separate the clusters.

Most populated clusters	**F3**	**F6**	**F7**
1	27.1 %	67.6%	86%
2	26.2%	26.5%	9.5%
3	10.8%	0.04%	3.4%
4	6.4 %	-	0.4%
5	6%	-	-

2.3.4 Hydrogen bond analysis from MD trajectory

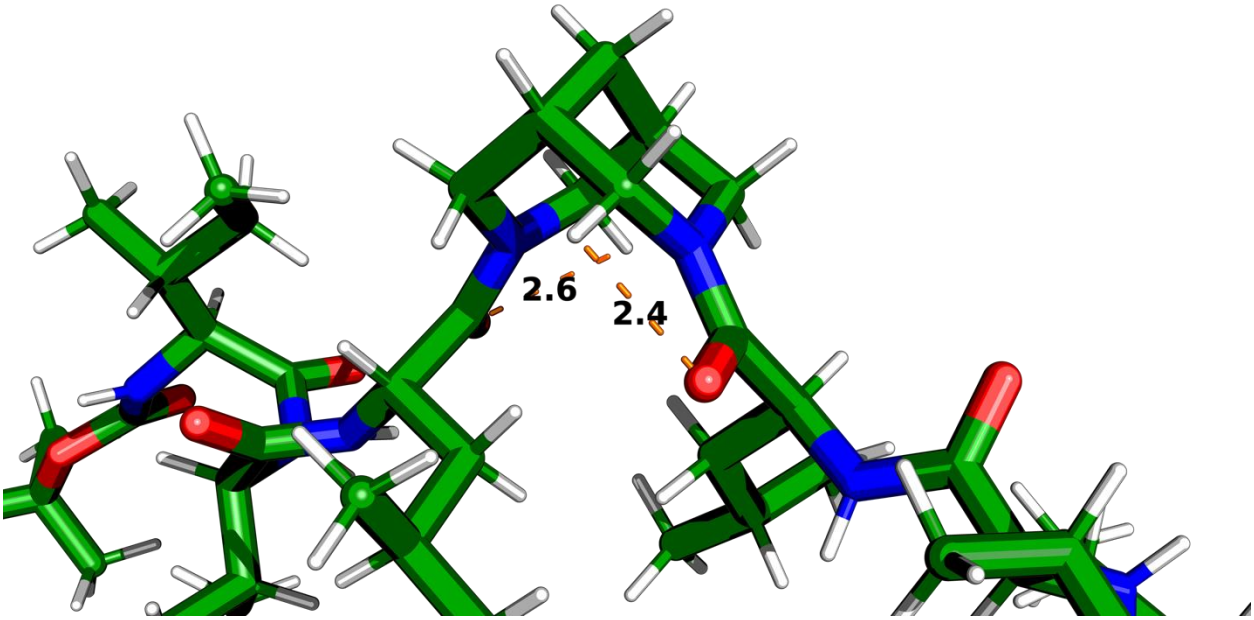

Fig. S12a: Orange dashed lines depict the C−H···O interactions between the bisipdine equatorial hydrogens (donor) and the carbonyl oxygen of the adjacent Leu residues (acceptor) in the central structure of the most populated cluster for the *anti*-form of **F3** in $CHCl_3$ obtained from the stable portion of MD trajectory. A distance cutoff of 2.7Å and a minimum angle criterion of 90° between the donor and acceptor atoms is considered for the formation of a C−H···O bonds.

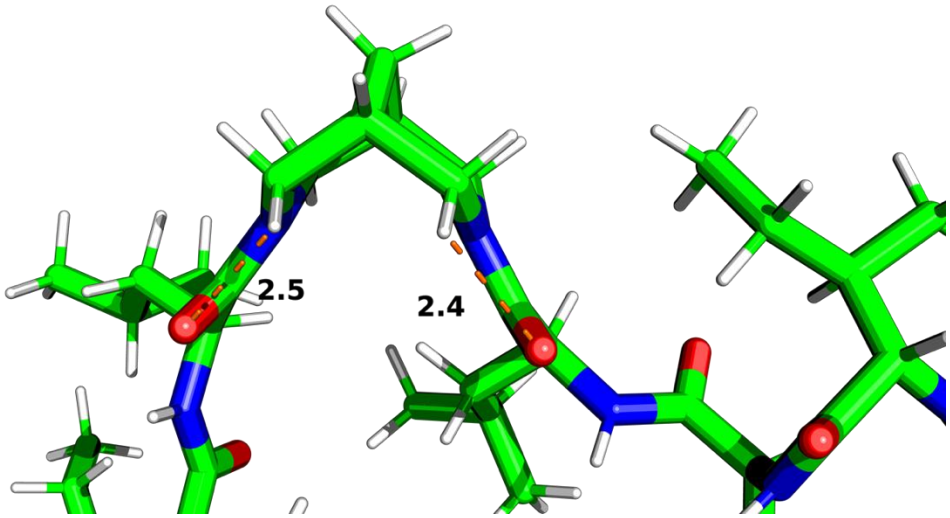

Fig. S12b: C−H···O bonds in the *syn* form of **F3** obtained from simulations in $CHCl_3$ solvent are shown by dashed lines between the bisipdine equatorial hydrogens (donor) and the carbonyl oxygen of the adjacent Leu (acceptor).

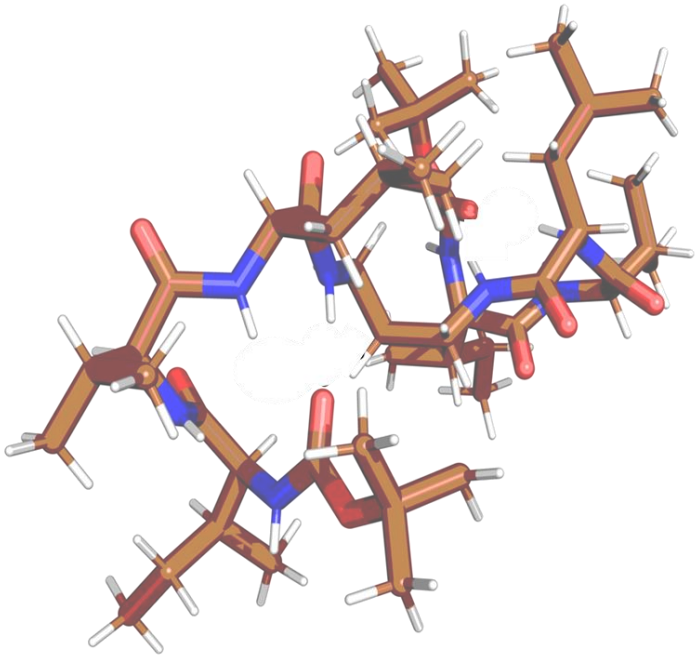

Fig. S12c: The central structure of the most populated clusters of **F7** simulated in $CHCl_3$ solvent.

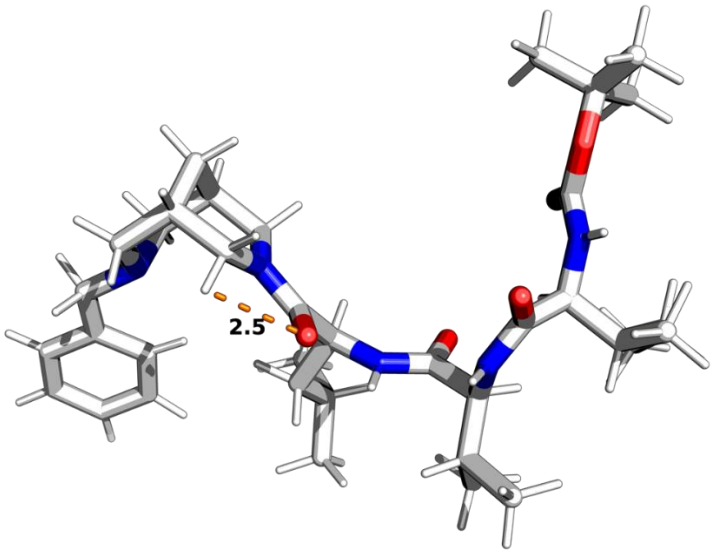

Fig. S12d: The central structure of the most populated clusters of **F6** simulated in $CHCl_3$ solvent shows a C−H···O bond between the equatorial hydrogens (donor) of the bispidine linker and the carbonyl oxygen of the adjacent Leu (acceptor) as observed in **F3**.

Table S10: C−H···O bond distances based on X-ray and MD simulation.

Compound Name	Average bond distance between Leu carbonyl oxygen and bispidine equatorial hydrogen
F1	2.4 Å
F3 (*Anti* form) **F3 (*Syn* form)**	2.5 Å 2.5 Å
F6	2.5 Å

Table S11: C−H···O hydrogen bonds between the linker and the carbonyl oxygen of Leu are compared for the bispidine linker (**F3**, **F6**) and diaminopropane linker (**F7**). The effective number of C−H···O bonds formed per tripeptide arm is listed in the top row. The last row is the trajectory average for the number of intramolecular hydrogen bonds considering N, O atoms as acceptors and NH, OH atoms as donors. The presence of C−H···O bonds in **F3** and **F6** is hypothesized in conferring β strand secondary structure stability. The absence of C−H···O bonds as observed in **F7** and a "hydrophilic collapse" arising from intramolecular hydrogen bonds in a nonpolar solvent ($CHCl_3$) leads to a poor β character as shown in **Table S8**.

	F3	**F6**	**F7**
C-H---O per arm **(**$d_{\mathrm{H-O}} < 2.7$Å $\angle CHO > 90°$**)**	0.77	0.71	0.27
Intramolecular H bonds ($d_{\mathrm{D-A}} < 3.5$Å $\angle DHA > 135°$**)**	0.28	0	

2.3.5 NOE correlations

gmx rmsdist was used to obtain ^{1}H two-dimensional Nuclear Overhauser Effect Spectroscopy (2D-NOESY) correlations for hydrogen atoms from the equilibrium portion of single molecule trajectories of **F3** and **F6** in $CHCl_3$ at 298K.

2.3.5.1 NOE correlations in F3

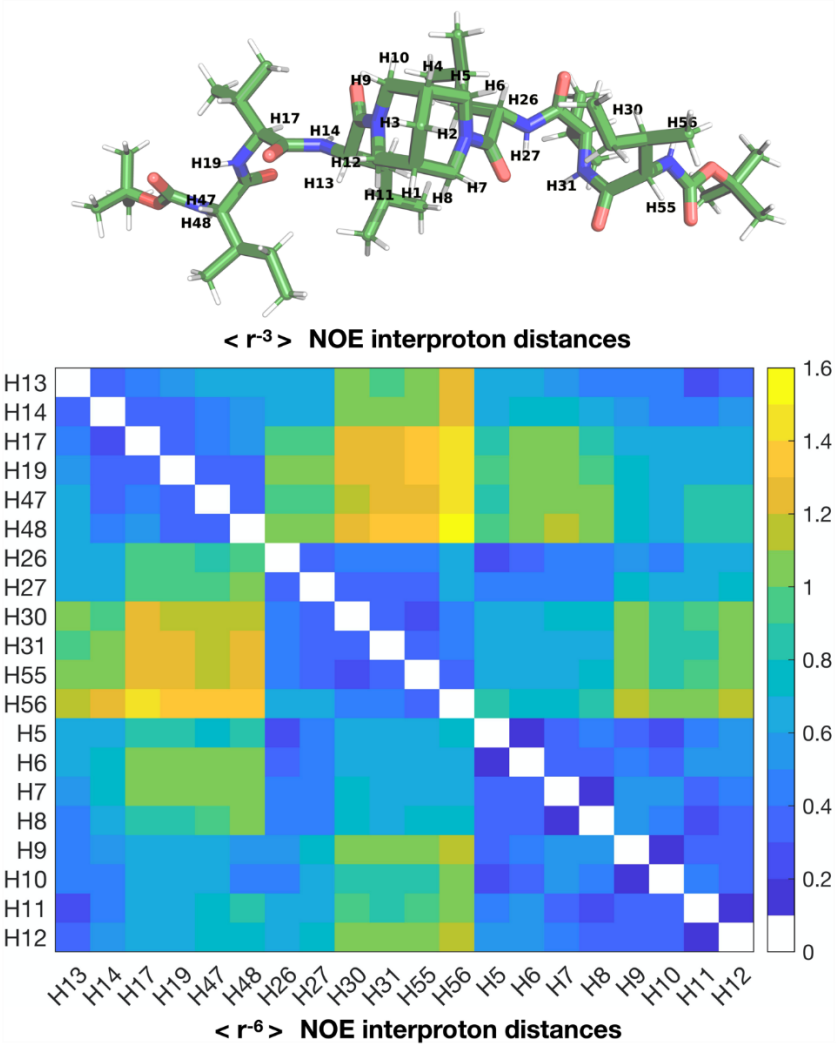

Fig. S13a The distance matrix represents the r^{-3} and r^{-6} averaged interproton distances in the upper and lower triangular matrices respectively for the hydrogen atoms of **F3**.

2.3.5.2 NOE correlations in F6

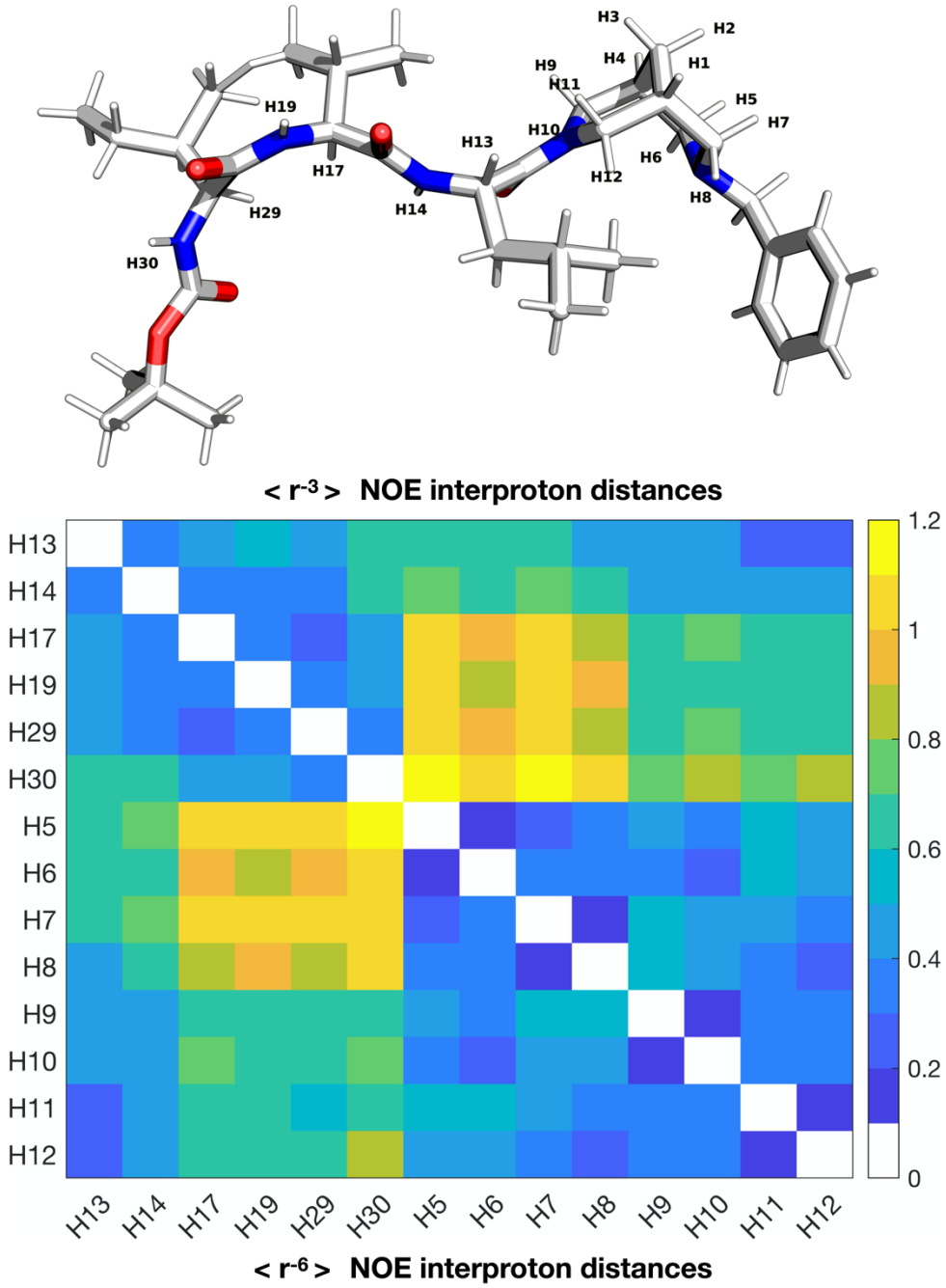

Fig. S13b: The distance matrix represents the r^{-3} and r^{-6} averaged interproton distances in the upper and lower triangular matrices respectively for the hydrogen atoms of bispidine linker and backbone residues of **F6**.

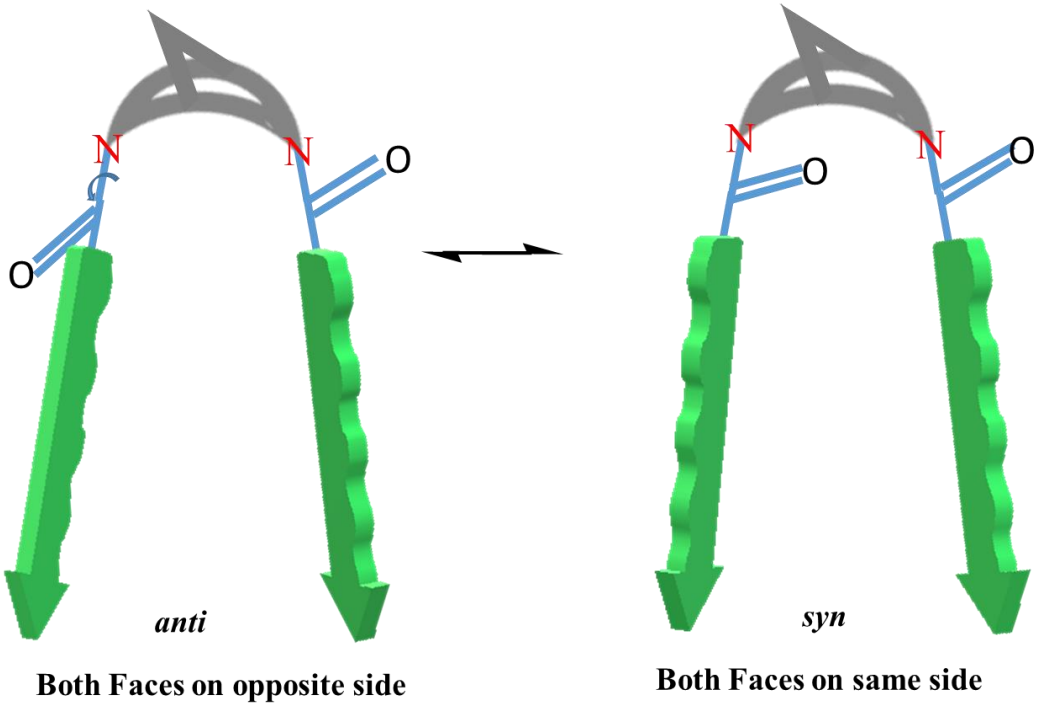

Fig. S14: Cartoon representation of β-strand – turn – β-strand (β-arch) showing the faces of two isolated β-strands in opposite side (*anti* form) and in same direction (*syn* form).

2.3.5 Potential energy surface in the space of relative orientation of bispidine strands

We scanned the potential energy surface of the **F1** for every five degree change in the dihedral of the carbonyl group with the linker connecting both strands. ORCA quantum chemistry package was used for geometry optimization[8] at the DFT level for every dihedral configuration using the default convergence criteria (here a convergence of < 0.1 kT between successive geometry optimization steps for all structures was achieved). CAM-B3LYP/6-31G* functional basis set was applied for the DFT calculation and the default Quasi-Newton BFGS optimization algorithm was used for geometry optimization. We observed the presence of a stable *anti* conformation as confirmed from the crystal structure of **F1** and its interconversion to the *syn* form (**Fig. S14**) as verified from ^{1}H NMR spectra of **F1-F3** molecules (**Table S1**).

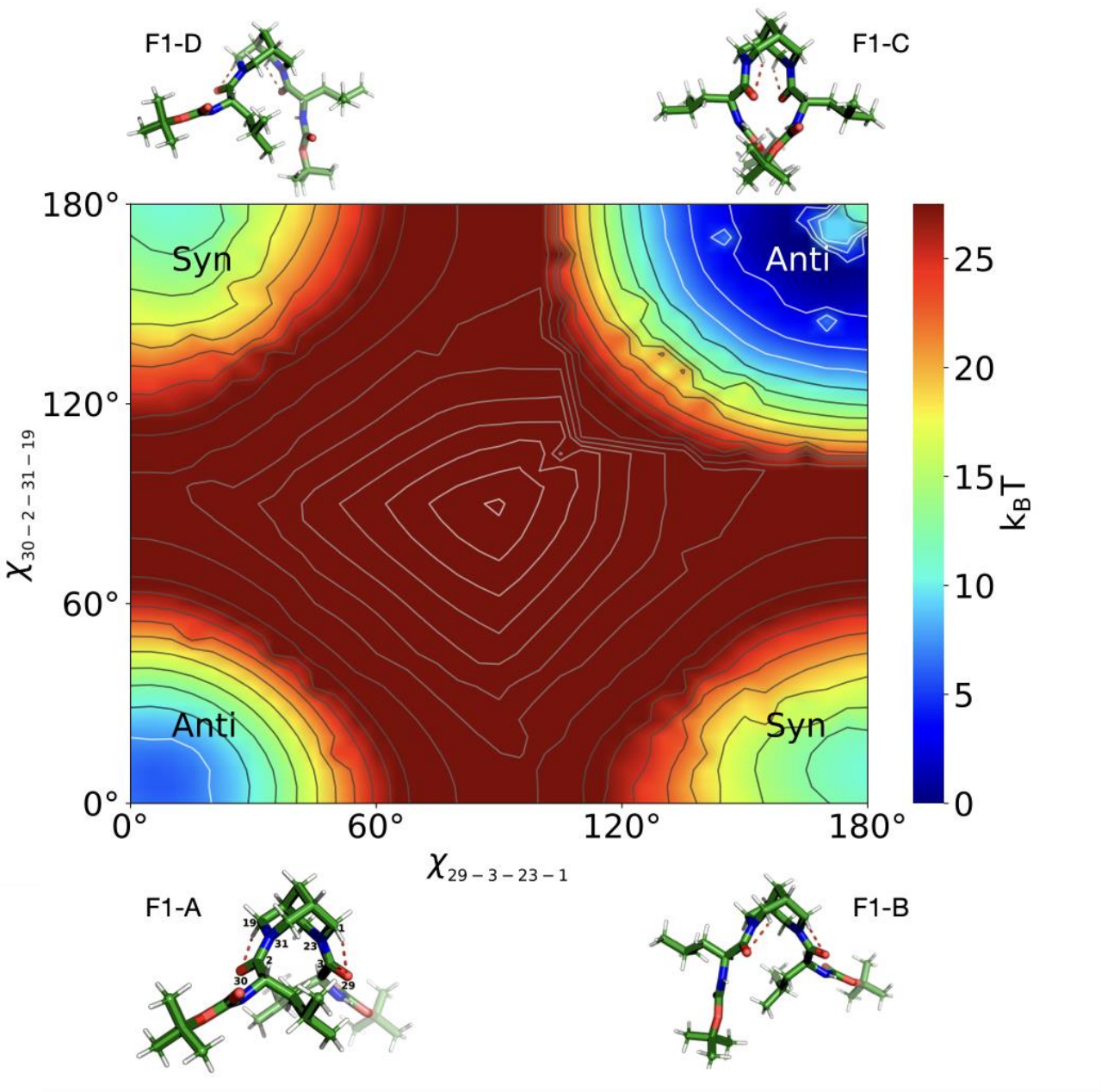

Fig. S15: Two-dimensional potential energy surface of **F1** in different strand orientations is plotted relative to the most stable structure (*anti*). The *syn*- and *anti*- forms of the bispidine linker represent its most stable states. Four lowest energy structures are displayed adjacent to their strand configurations in the potential energy map. The structures show C-H---O bonds (displayed in red) on both sides of the linker. Consequently, the adjacent leucine residues adopt a β secondary structure with Φ greater than 150° (**Table S12**).

Table S12: Properties of **F1** determined from DFT based geometry optimization.

	C-H---O bonds ($d_{\mathrm{H-O}} <$ 2.7Å $\angle CHO > 90°$)	**Leu-ψ (deg)**	**Secondary structure (Leu)**
F1-A (*Anti*)	2	156	β
F1-B (*Syn*)	2	161	β
F1-C (*Anti*)	2	153	β
F1-D (*Syn*)	2	162	β

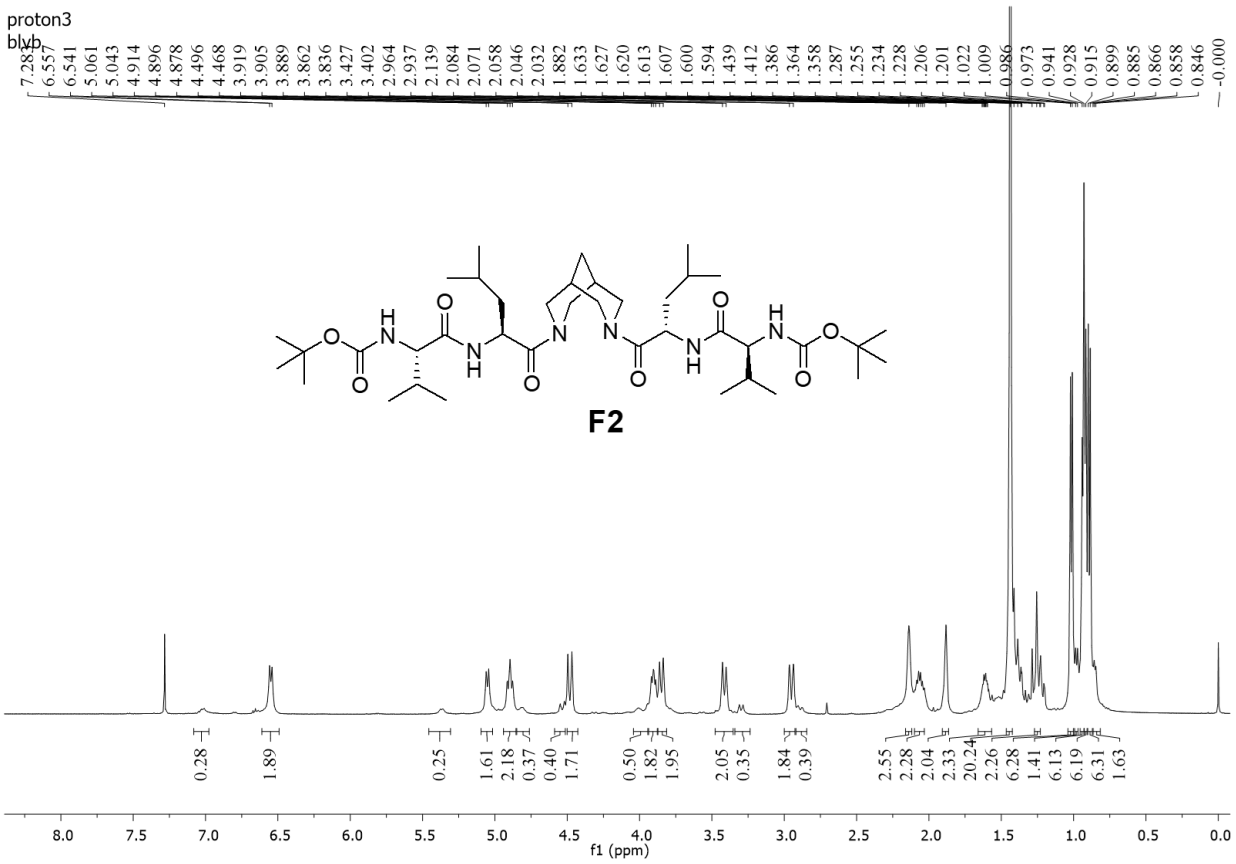

^{1}H NMR ($CDCl_3$, 500 MHz) of **F2**

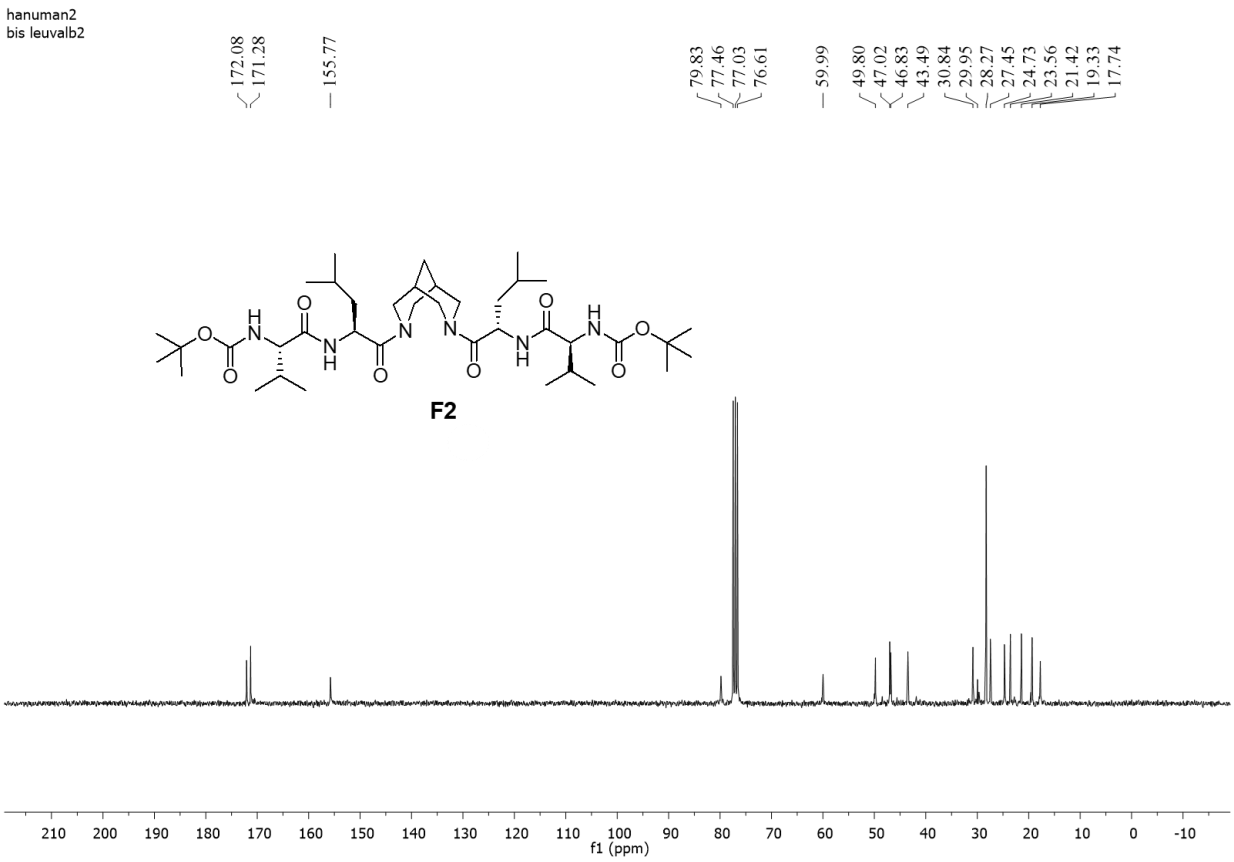

^{13}C NMR (75 MHz, $CDCl_3$) of **F2**

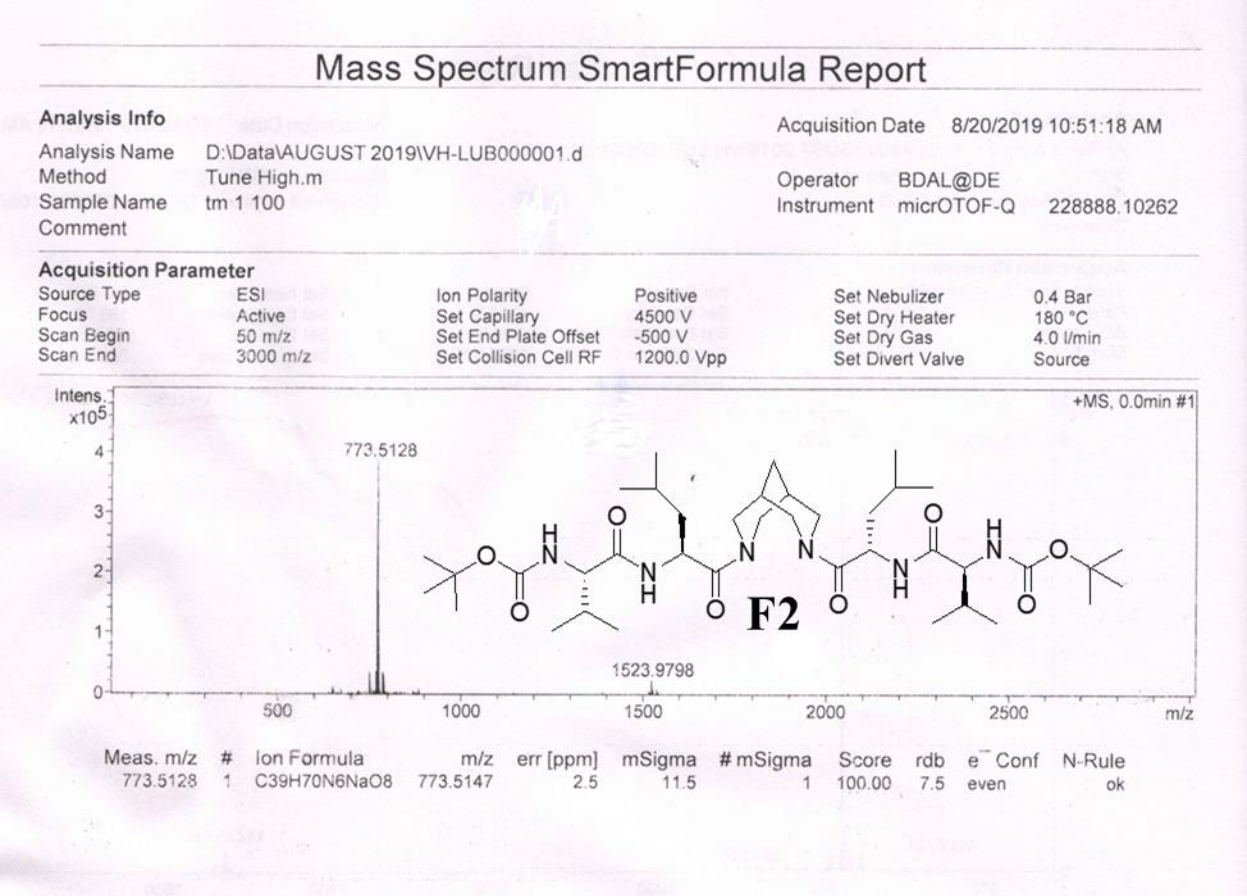
Mass Spectrum SmartFormula Report
Analysis Info
Analysis Name D:\Data\AUGUST 2019\VH-LUB000001.d
Method Tune High.m
Sample Name tm 1 100
Comment
Acquisition Date 8/20/2019 10:51:18 AM
Operator BDAL@DE
Instrument micrOTOF-Q 228888.10262
Acquisition Parameter
Source Type ESI
Focus Active
Scan Begin 50 m/z
Scan End 3000 m/z
Ion Polarity Positive
Set Capillary 4500 V
Set End Plate Offset -500 V
Set Collision Cell RF 1200.0 Vpp
Set Nebulizer 0.4 Bar
Set Dry Heater 180 °C
Set Dry Gas 4.0 l/min
Set Divert Valve Source
Intens.
x10^5
+MS, 0.0min #1
773.5128
1523.9798
F2
m/z
Meas. m/z # Ion Formula m/z err [ppm] mSigma # mSigma Score rdb e⁻ Conf N-Rule
773.5128 1 C39H70N6NaO8 773.5147 2.5 11.5 1 100.00 7.5 even ok

HRMS of **F2**

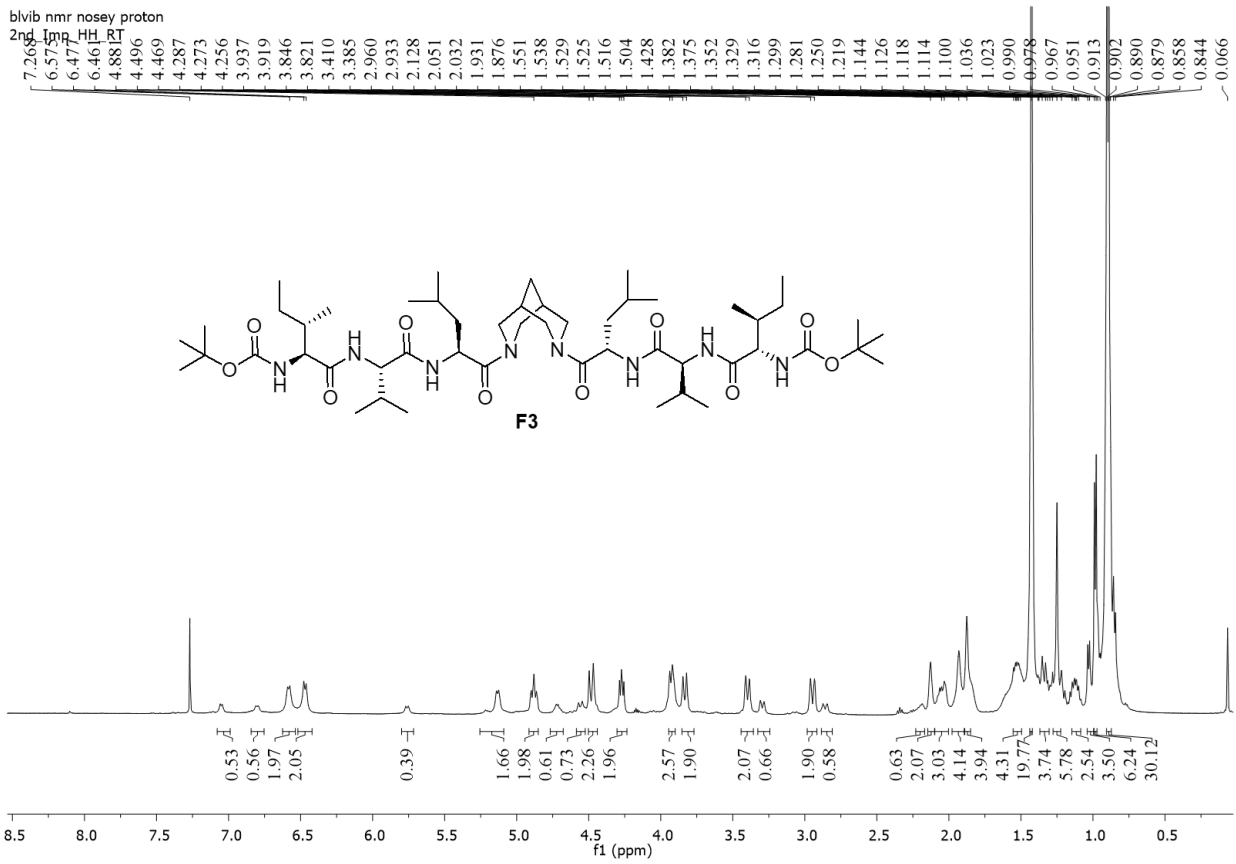

^{1}H NMR ($CDCl_3$, 500 MHz) of **F3**

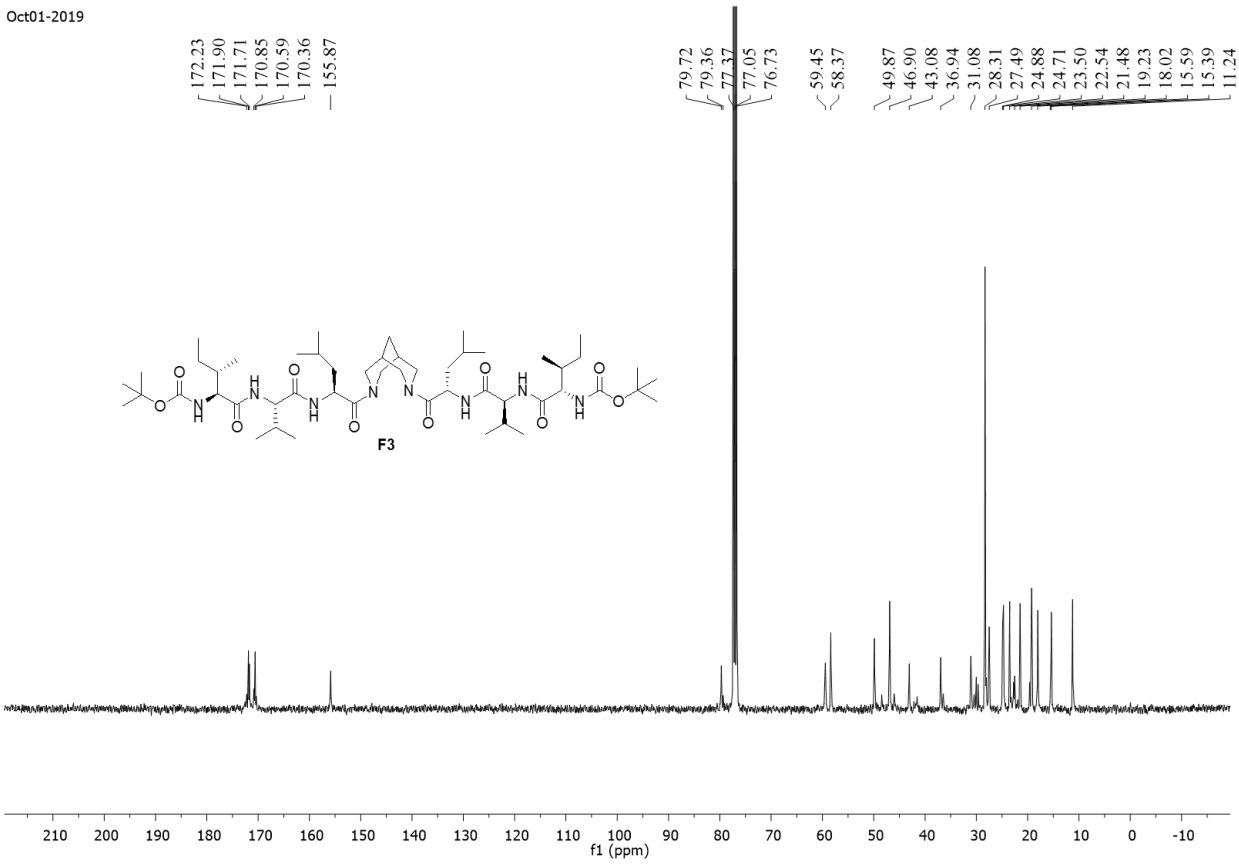

^{13}C NMR (100 MHz, $CDCl_3$) of **F3**

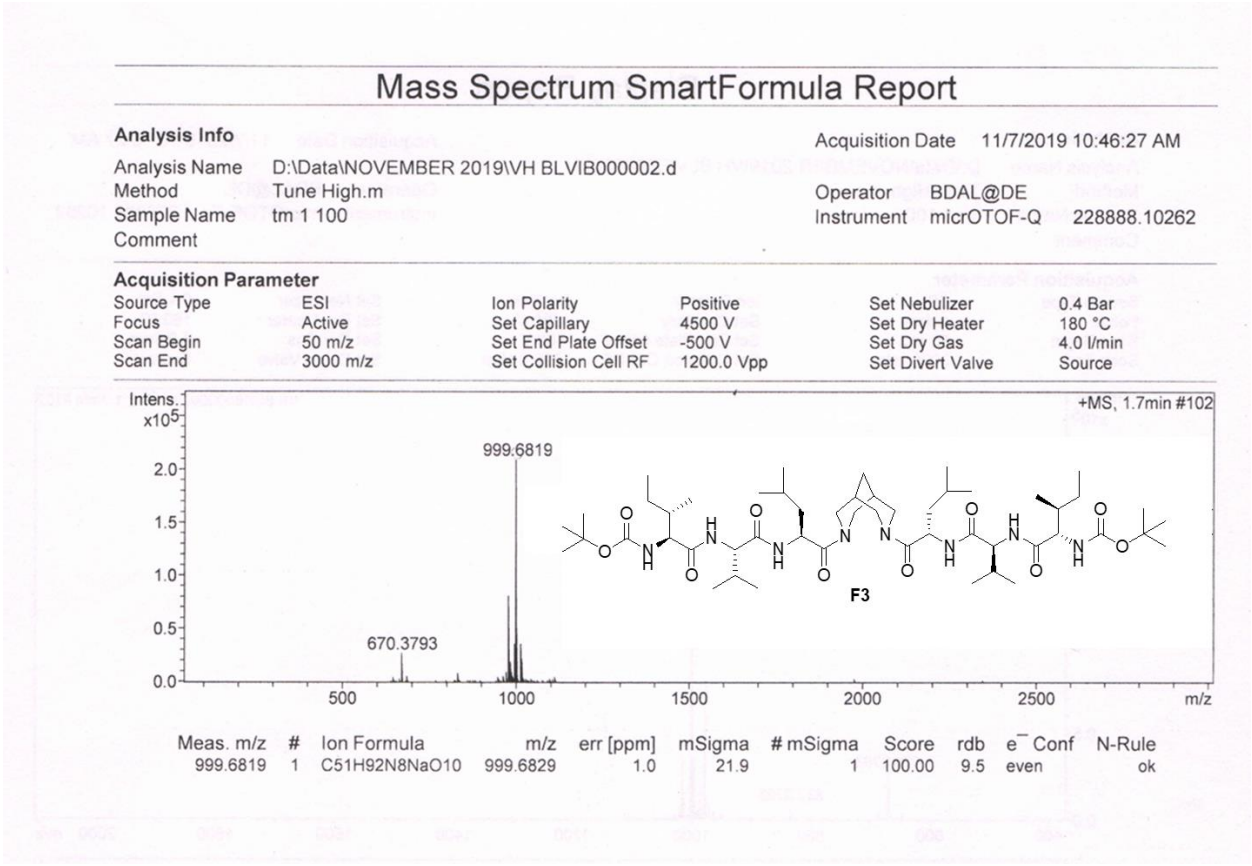
Mass Spectrum SmartFormula Report
Analysis Info
Acquisition Date 11/7/2019 10:46:27 AM
Analysis Name D:\Data\NOVEMBER 2019\VH BLVIB000002.d
Method Tune High.m
Operator BDAL@DE
Sample Name tm 1 100
Instrument micrOTOF-Q 228888.10262
Comment
Acquisition Parameter
Source Type ESI
Ion Polarity Positive
Set Nebulizer 0.4 Bar
Focus Active
Set Capillary 4500 V
Set Dry Heater 180 °C
Scan Begin 50 m/z
Set End Plate Offset -500 V
Set Dry Gas 4.0 l/min
Scan End 3000 m/z
Set Collision Cell RF 1200.0 Vpp
Set Divert Valve Source
Intens.
x10^5
+MS, 1.7min #102
999.6819
670.3793
F3
m/z
Meas. m/z # Ion Formula m/z err [ppm] mSigma # mSigma Score rdb e⁻ Conf N-Rule
999.6819 1 C51H92N8NaO10 999.6829 1.0 21.9 1 100.00 9.5 even ok

HRMS of **F3**

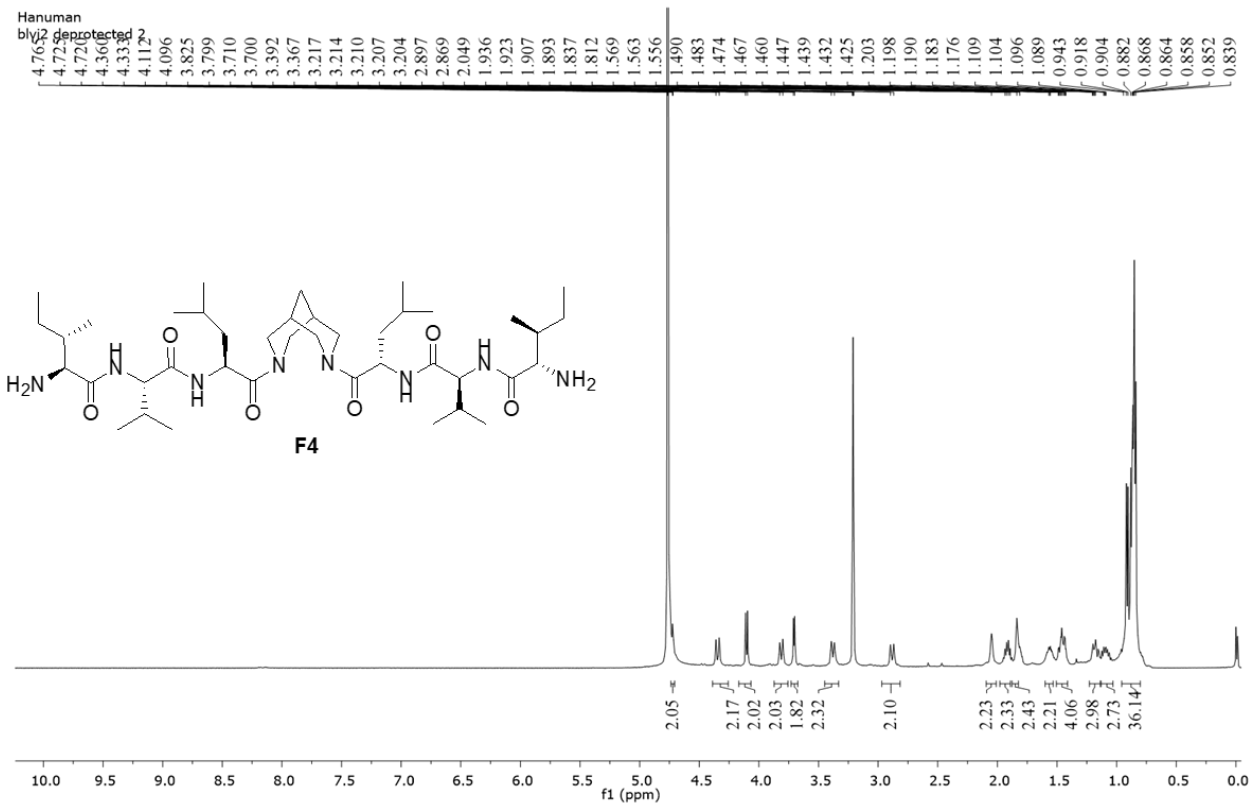

^{1}H NMR (CD_3OD, 500 MHz) of **F4**

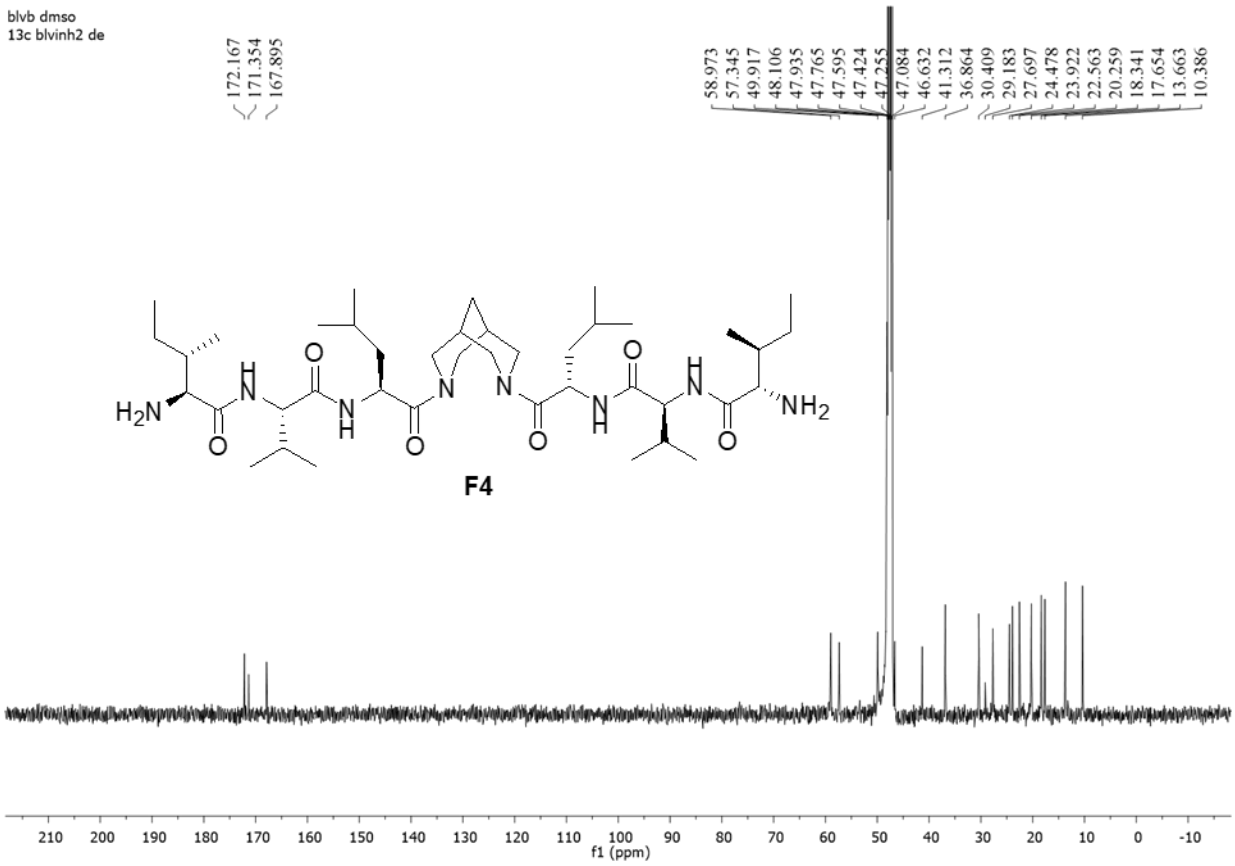

^{13}C NMR (CD_3OD, 125 MHz) of **F4**

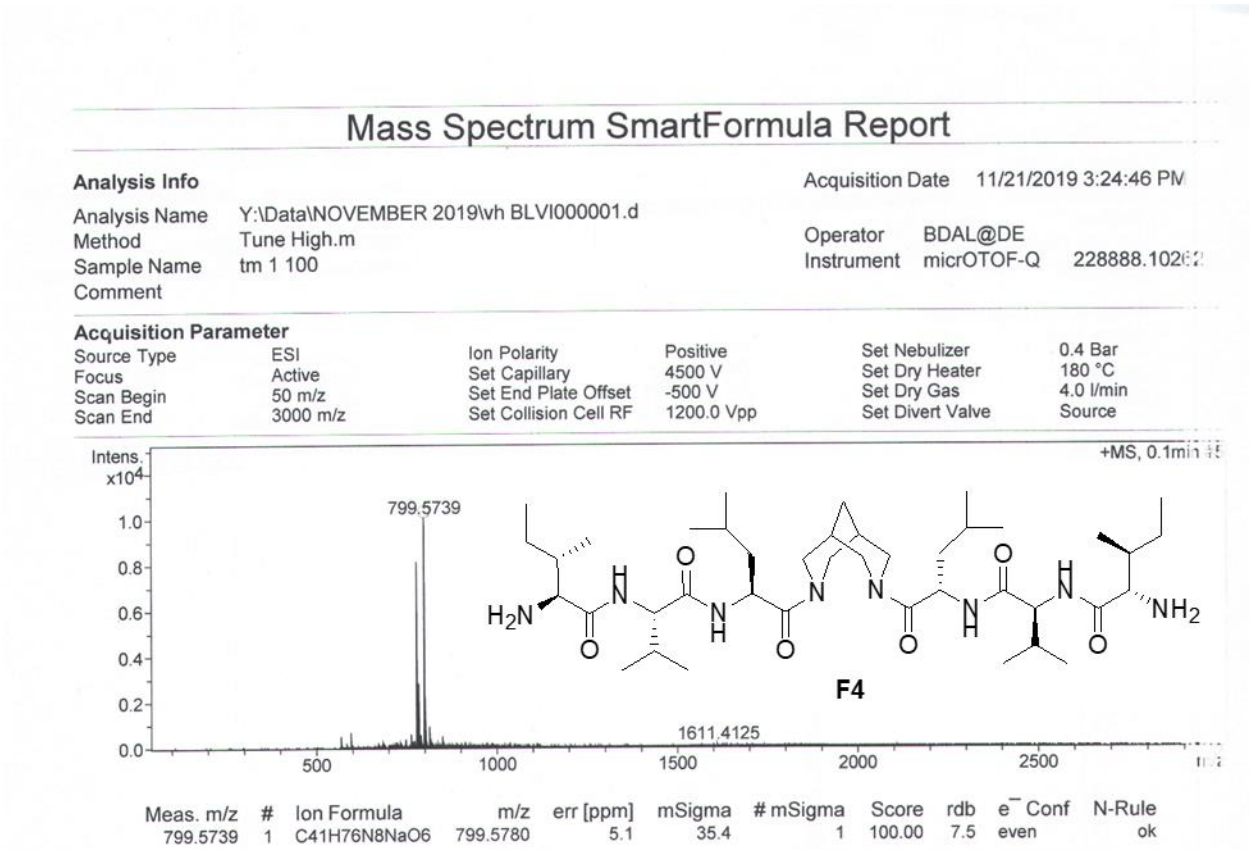
Mass Spectrum SmartFormula Report
Analysis Info
Acquisition Date 11/21/2019 3:24:46 PM
Analysis Name Y:\Data\NOVEMBER 2019\vh BLVI000001.d
Method Tune High.m
Sample Name tm 1 100
Comment
Operator BDAL@DE
Instrument micrOTOF-Q
Acquisition Parameter
Source Type ESI
Focus Active
Scan Begin 50 m/z
Scan End 3000 m/z
Ion Polarity Positive
Set Capillary 4500 V
Set End Plate Offset -500 V
Set Collision Cell RF 1200.0 Vpp
Set Nebulizer 0.4 Bar
Set Dry Heater 180 °C
Set Dry Gas 4.0 l/min
Set Divert Valve Source
Intens.
x10^4
+MS, 0.1min
799.5739
1611.4125
F4
Meas. m/z # Ion Formula m/z err [ppm] mSigma # mSigma Score rdb e¯ Conf N-Rule
799.5739 1 C41H76N8NaO6 799.5780 5.1 35.4 1 100.00 7.5 even ok

HRMS of **F4**

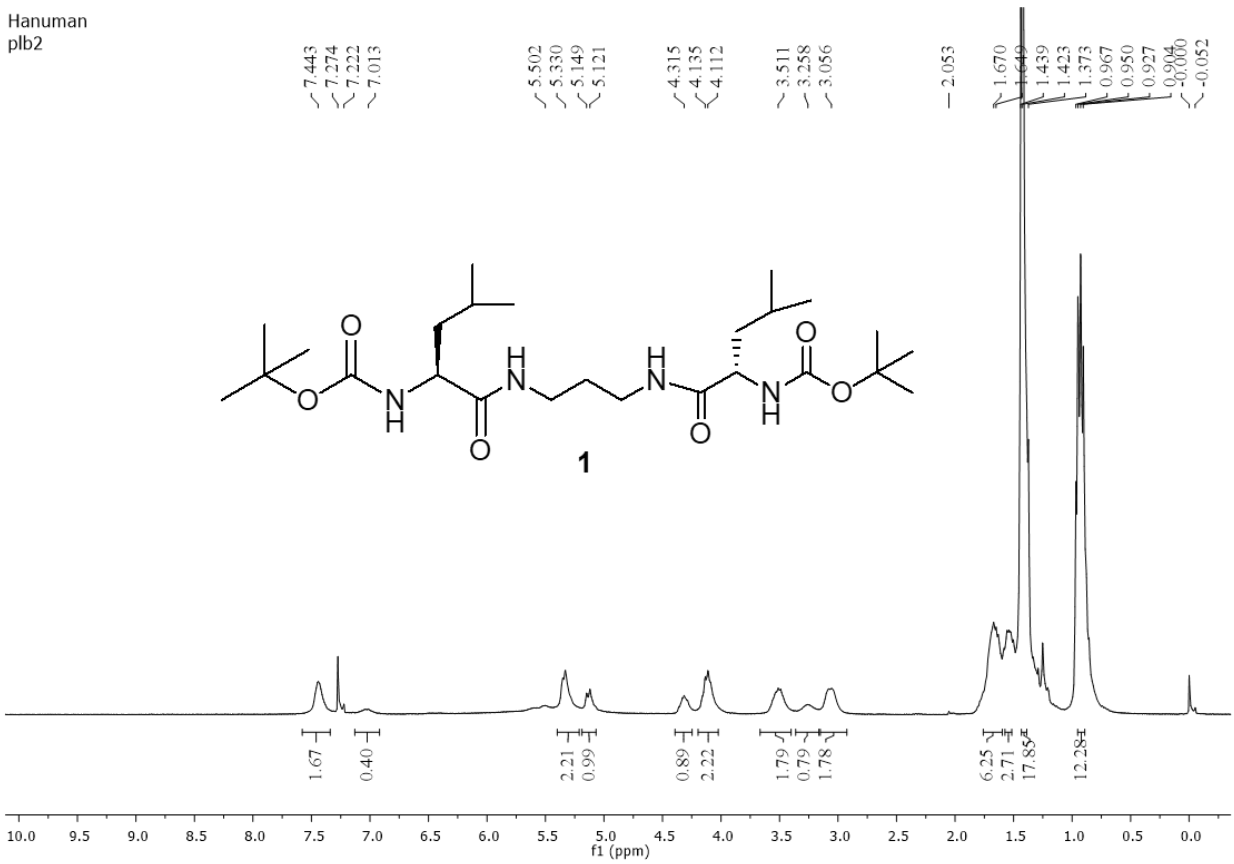

^{1}H NMR ($CDCl_3$, 300 MHz) of **1**

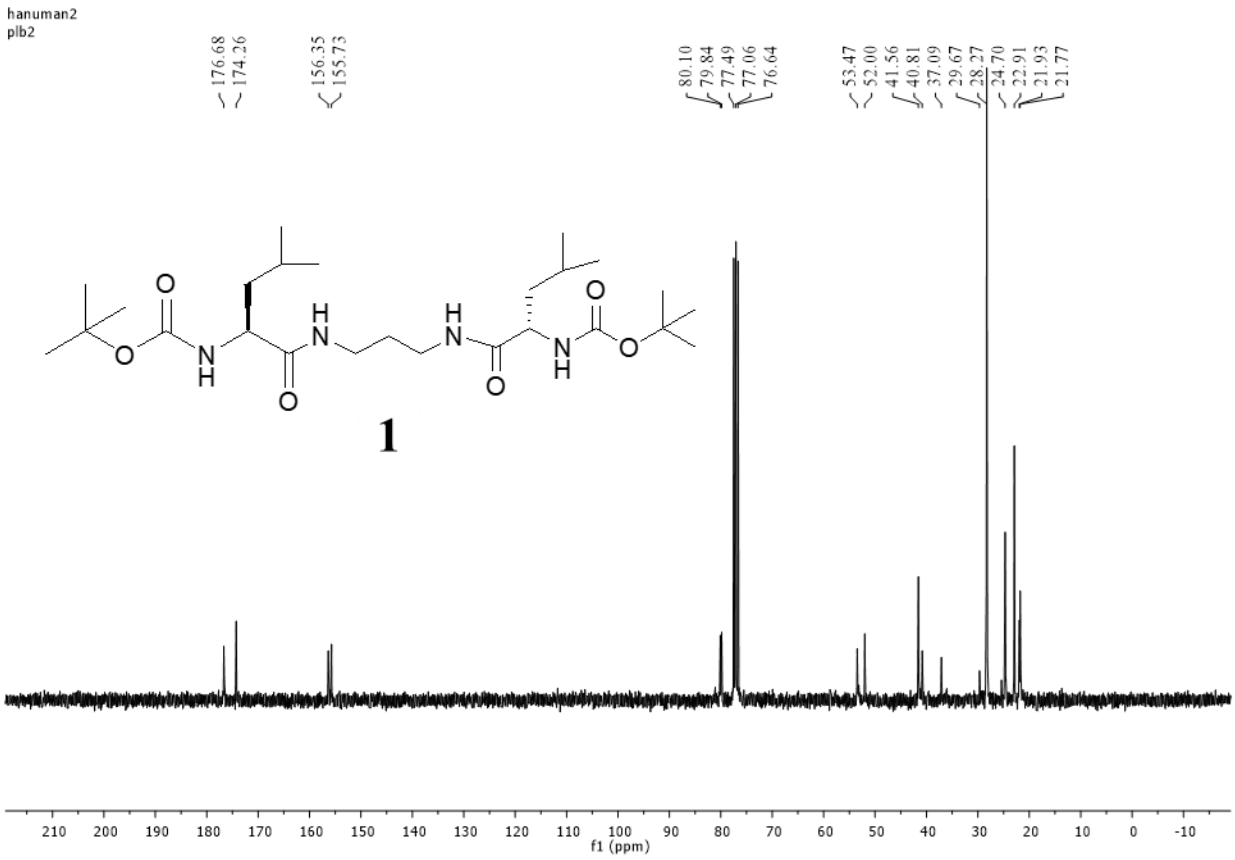

^{13}C NMR (75 MHz, $CDCl_3$) of **1**

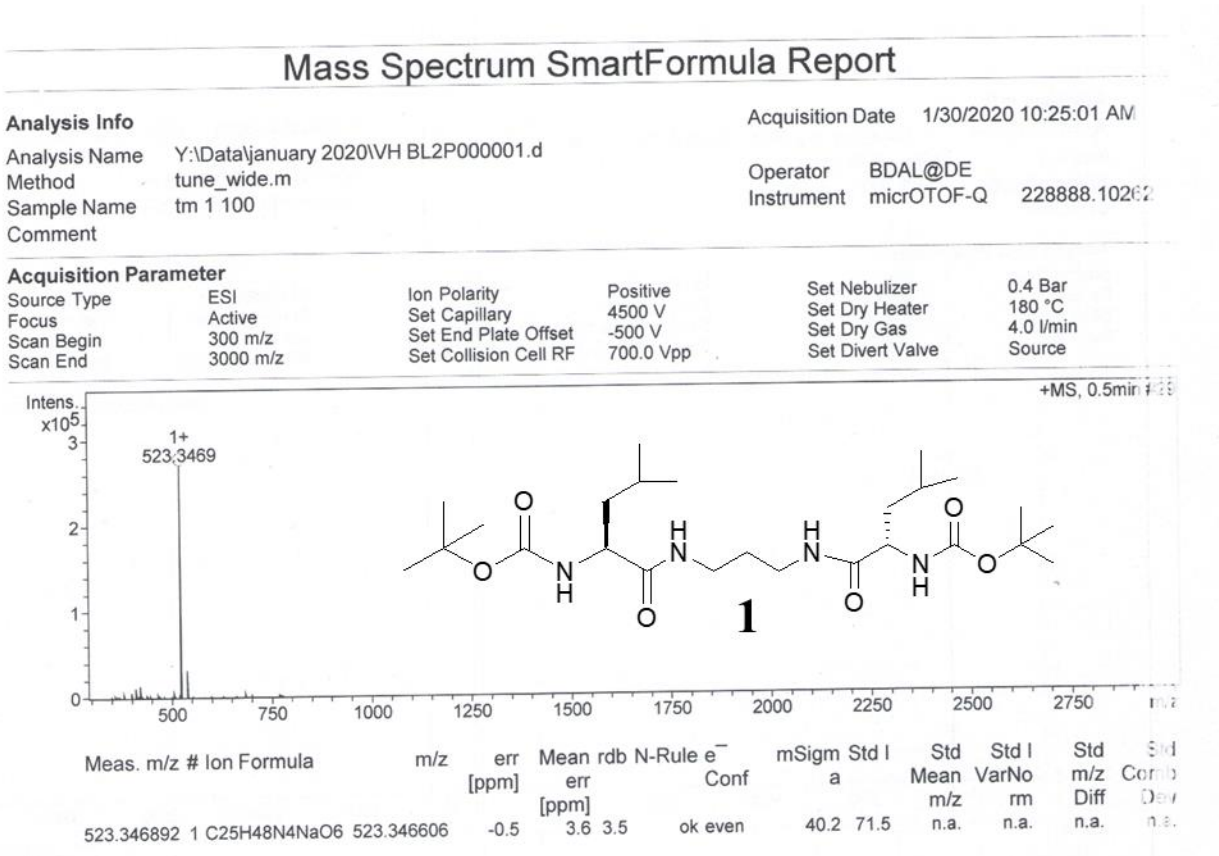
Mass Spectrum SmartFormula Report
Analysis Info
Acquisition Date 1/30/2020 10:25:01 AM
Analysis Name Y:\Data\january 2020\VH BL2P000001.d
Method tune_wide.m
Sample Name tm 1 100
Comment
Operator BDAL@DE
Instrument micrOTOF-Q
Acquisition Parameter
Source Type ESI
Focus Active
Scan Begin 300 m/z
Scan End 3000 m/z
Ion Polarity Positive
Set Capillary 4500 V
Set End Plate Offset -500 V
Set Collision Cell RF 700.0 Vpp
Set Nebulizer 0.4 Bar
Set Dry Heater 180 °C
Set Dry Gas 4.0 l/min
Set Divert Valve Source
+MS, 0.5min
Intens.
x10^5
1+
523.3469
1
Meas. m/z # Ion Formula m/z err [ppm] Mean err [ppm] rdb N-Rule e⁻ Conf mSigma Std I Std Mean m/z Std I VarNorm Std m/z Diff
523.346892 1 C25H48N4NaO6 523.346606 -0.5 3.6 3.5 ok even 40.2 71.5 n.a. n.a. n.a.

HRMS of **1**

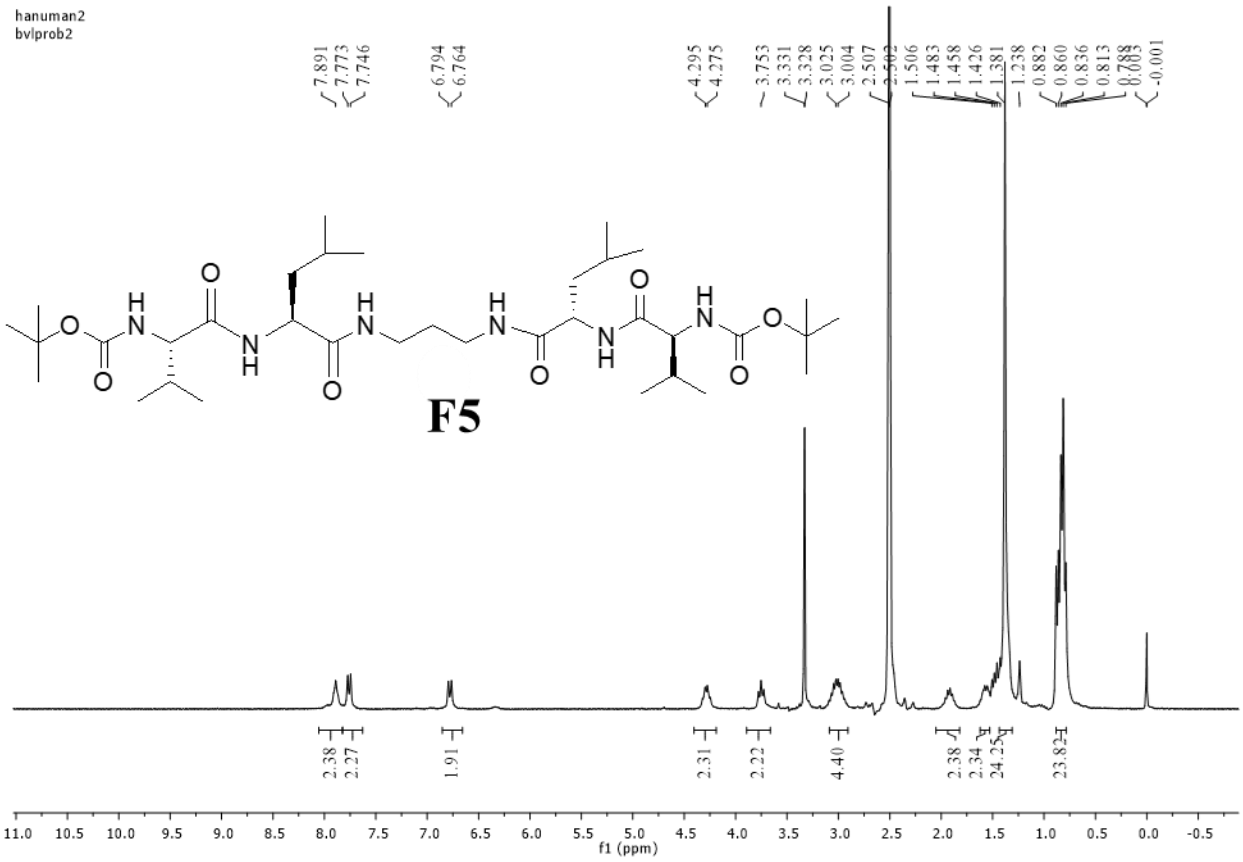

^{1}H NMR (DMSO-d_6, 300 MHz) of **F5**

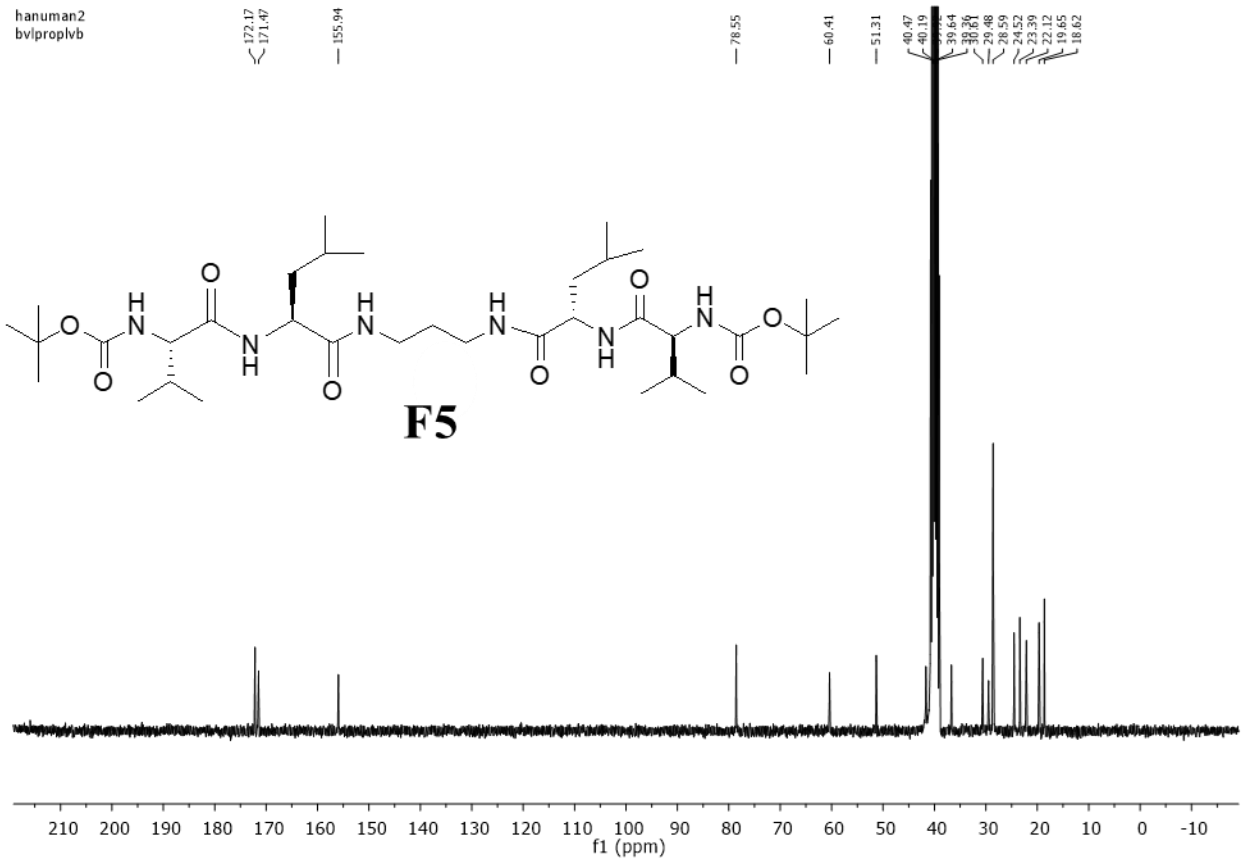

^{13}C NMR (75 MHz, DMSO-d_6) of **F5**

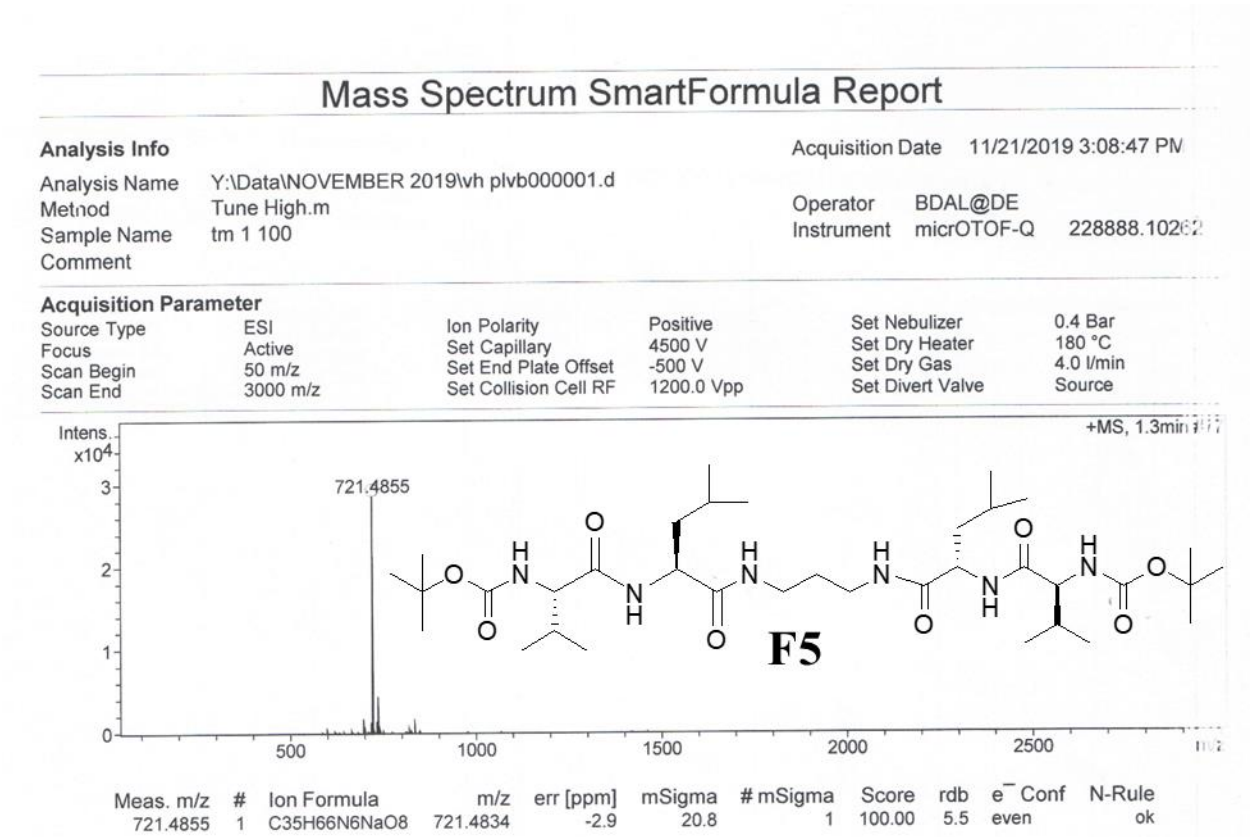
Mass Spectrum SmartFormula Report
Analysis Info
Acquisition Date 11/21/2019 3:08:47 PM
Analysis Name Y:\Data\NOVEMBER 2019\vh plvb000001.d
Method Tune High.m
Sample Name tm 1 100
Comment
Operator BDAL@DE
Instrument micrOTOF-Q 228888.10262
Acquisition Parameter
Source Type ESI
Focus Active
Scan Begin 50 m/z
Scan End 3000 m/z
Ion Polarity Positive
Set Capillary 4500 V
Set End Plate Offset -500 V
Set Collision Cell RF 1200.0 Vpp
Set Nebulizer 0.4 Bar
Set Dry Heater 180 °C
Set Dry Gas 4.0 l/min
Set Divert Valve Source
Intens.
x10^4
+MS, 1.3min
721.4855
F5
Meas. m/z # Ion Formula m/z err [ppm] mSigma # mSigma Score rdb e⁻ Conf N-Rule
721.4855 1 C35H66N6NaO8 721.4834 -2.9 20.8 1 100.00 5.5 even ok

HRMS of **F5**

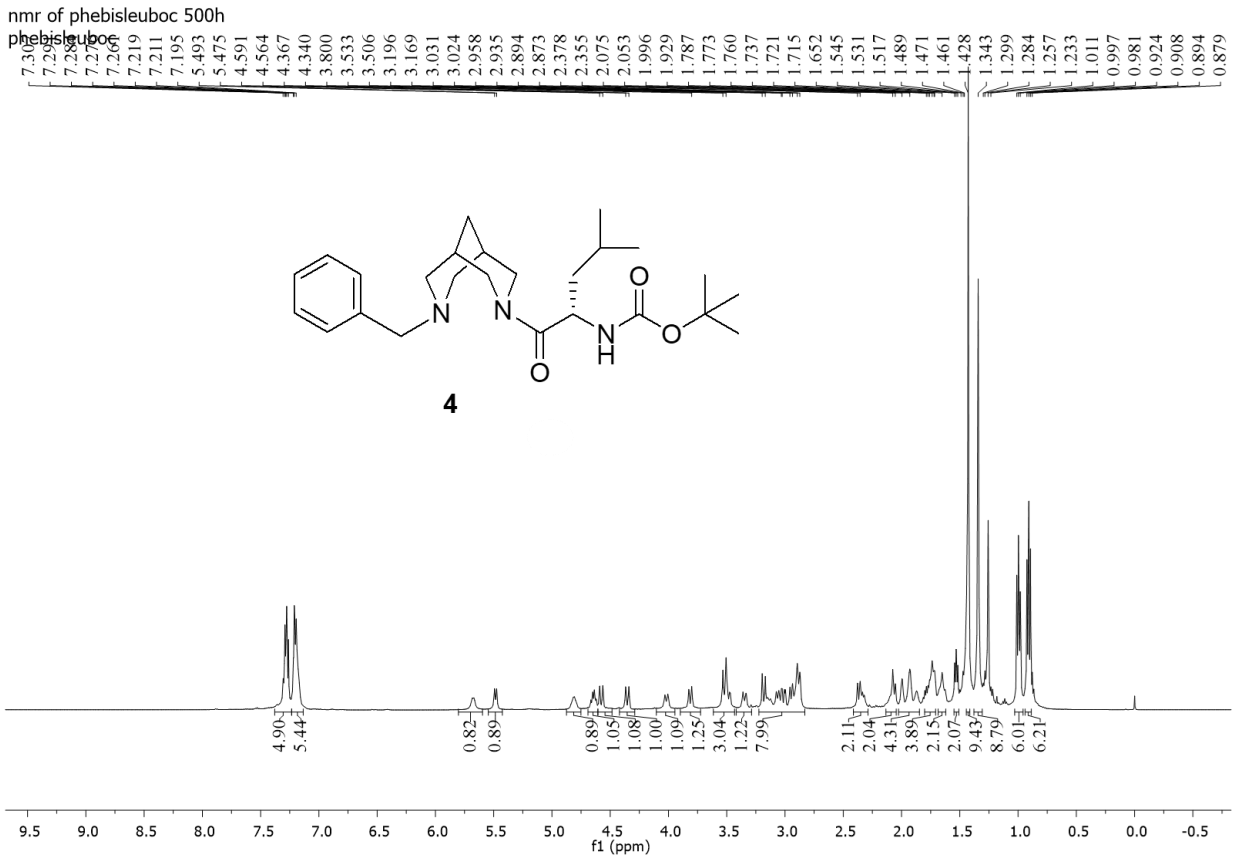

^{1}H NMR ($CDCl_3$, 500 MHz) of **4**

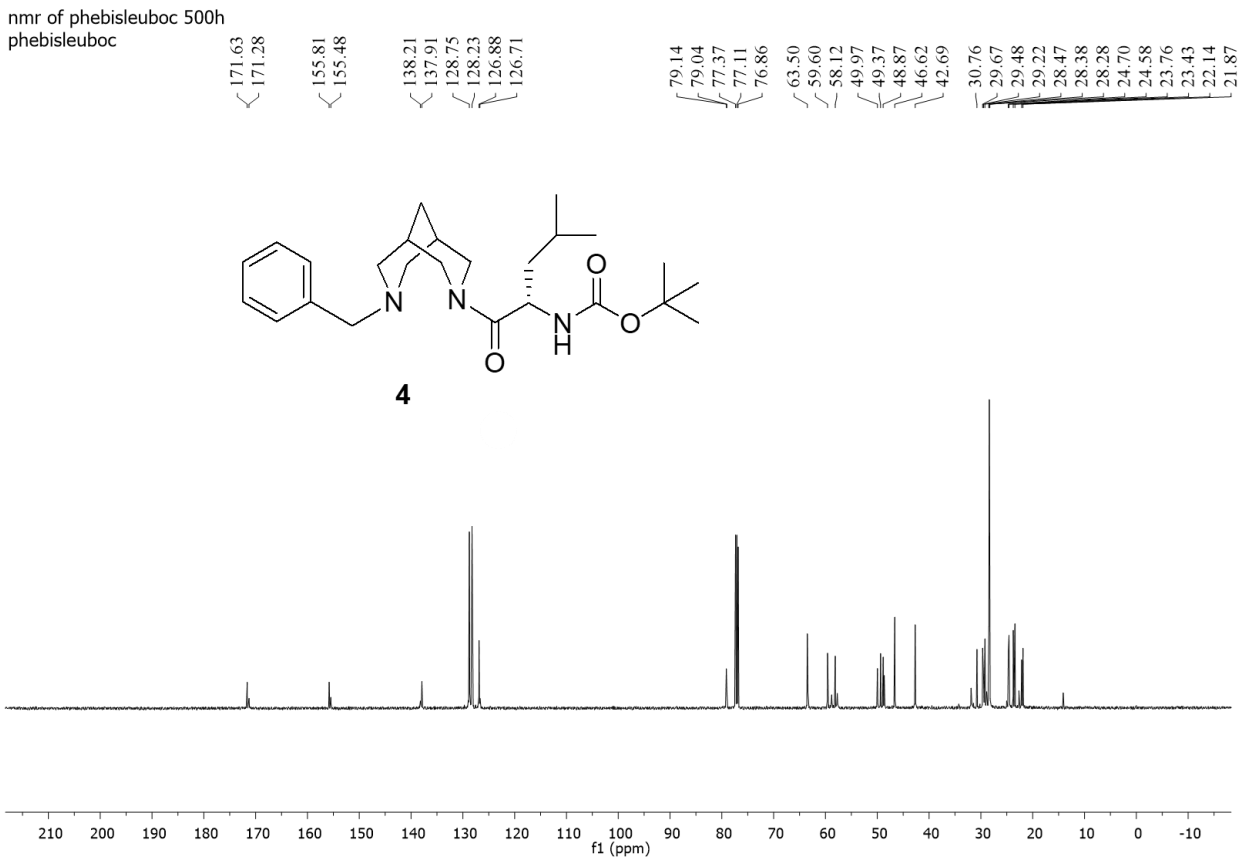

^{13}C NMR (125 MHz, $CDCl_3$) of **4**

Mass Spectrum SmartFormula Report

Analysis Info

Analysis Name	Y:\Data\FEBRUARY 2021\VH PHEBLB000001.d	Acquisition Date	02/26/21 3:40:03 PM
Method	tune_wide.m	Operator	BDAL@DE
Sample Name	Sharma sir	Instrument	micrOTOF-Q 228888.10262
Comment			

Acquisition Parameter

Source Type	ESI	Ion Polarity	Positive	Set Nebulizer	0.4 Bar
Focus	Active	Set Capillary	4500 V	Set Dry Heater	180 °C
Scan Begin	300 m/z	Set End Plate Offset	-500 V	Set Dry Gas	4.0 l/min
Scan End	3000 m/z	Set Collision Cell RF	700.0 Vpp	Set Divert Valve	Source

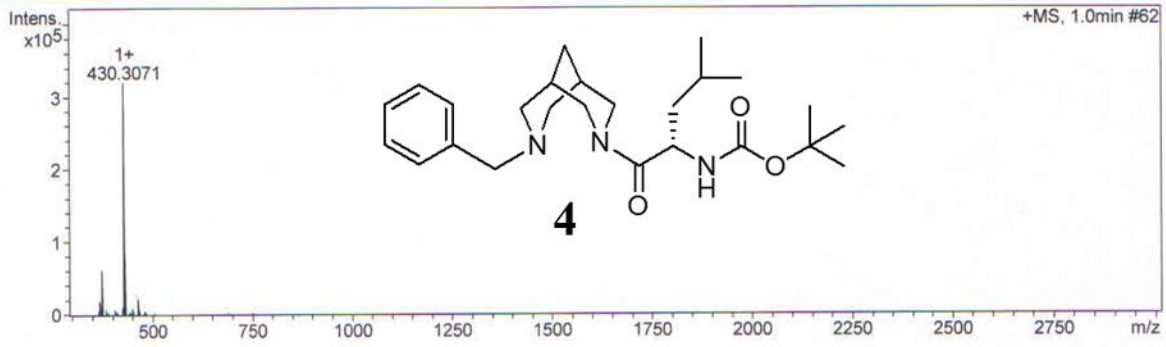

4

Meas. m/z	#	Ion Formula	m/z	err [ppm]	Mean err [ppm]	rdb	N-Rule	e⁻ Conf	mSigma	Std I a	Std Mean m/z	Std I VarNorm	Std m/z Diff	Std Comb Dev
430.307076	1	C25H40N3O3	430.306419	-1.5	3.7	7.5	ok	even	12.9	20.9	n.a.	n.a.	n.a.	n.a.

HRMS of **4**

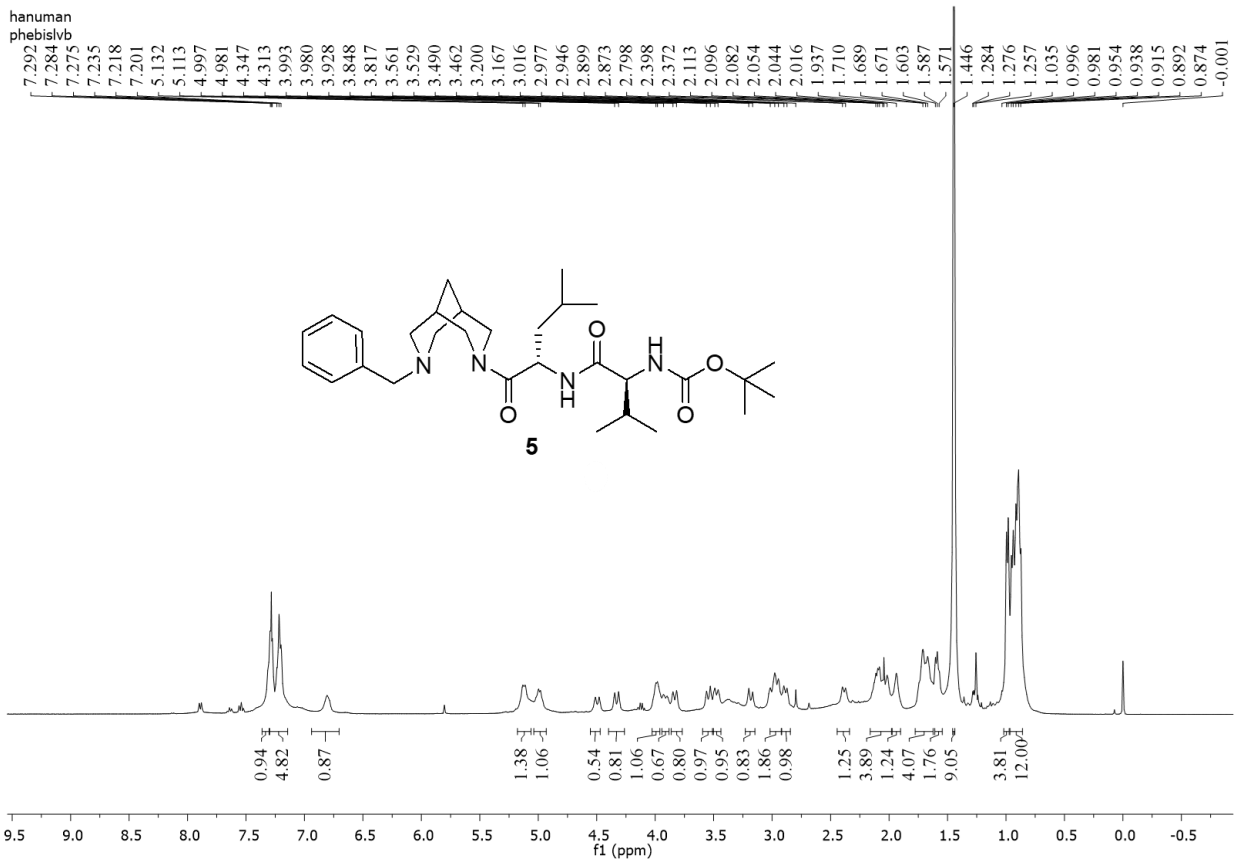

^{1}H NMR ($CDCl_3$, 400 MHz) of **5**

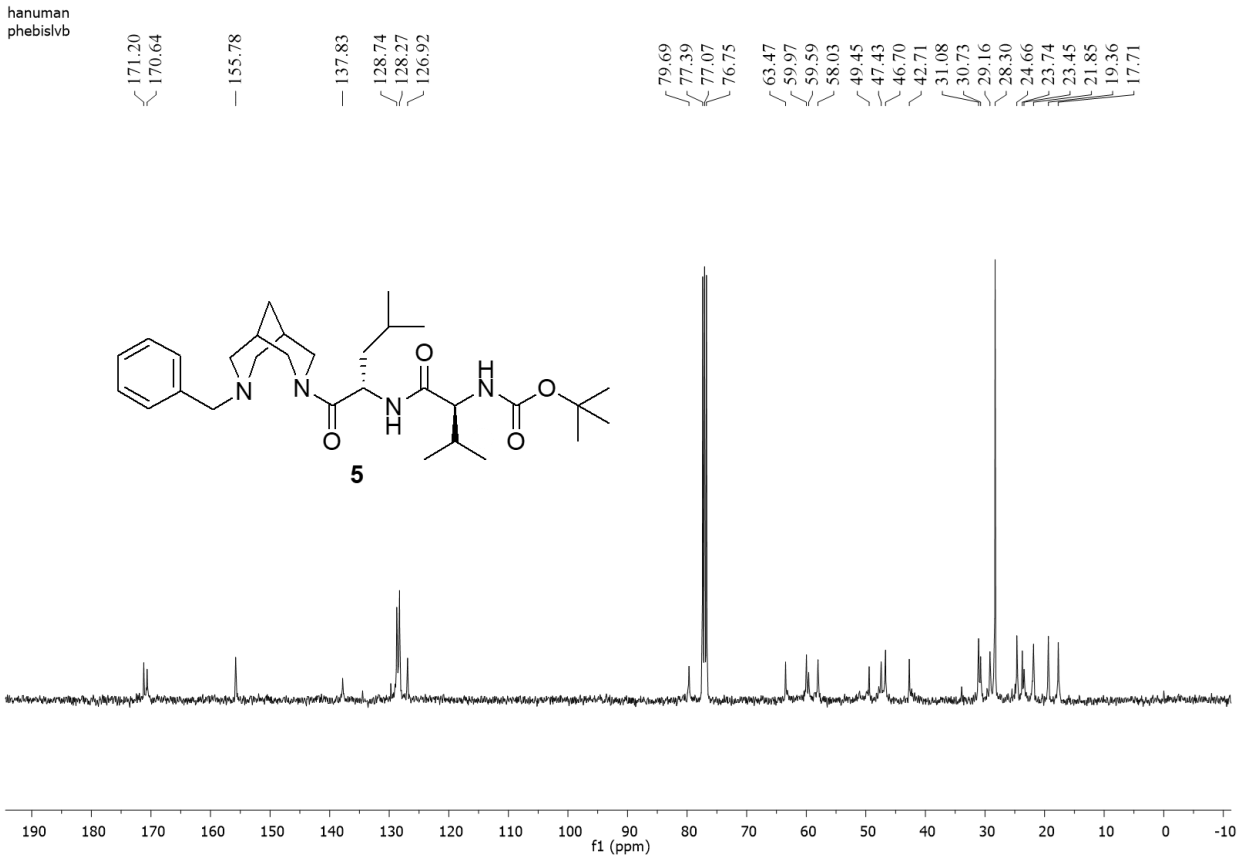

^{13}C NMR (100 MHz, $CDCl_3$) of **5**

Mass Spectrum SmartFormula Report

Analysis Info

Analysis Name	D:\Data\DECEMBER 2020\PBLVB000001.d	Acquisition Date	12/21/2020 3:42:26 PM
Method	tune_wide.m	Operator	BDAL@DE
Sample Name	tm 1 100	Instrument	micrOTOF-Q 228888.10262
Comment			

Acquisition Parameter

Source Type	ESI	Ion Polarity	Positive	Set Nebulizer	0.4 Bar
Focus	Active	Set Capillary	4500 V	Set Dry Heater	180 °C
Scan Begin	300 m/z	Set End Plate Offset	-500 V	Set Dry Gas	4.0 l/min
Scan End	3000 m/z	Set Collision Cell RF	700.0 Vpp	Set Divert Valve	Source

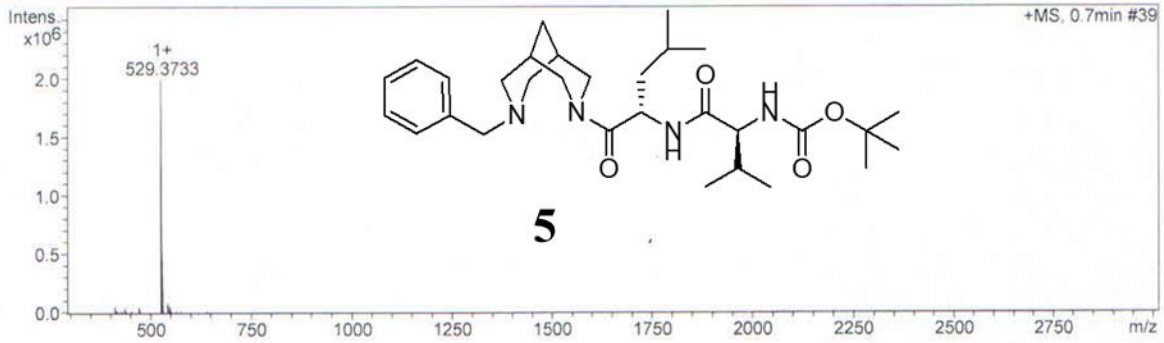

5

Meas. m/z	#	Ion Formula	m/z	err [ppm]	Mean err [ppm]	rdb	N-Rule	e⁻ Conf	mSigma	Std I	Std Mean m/z	Std I VarNorm	Std m/z Diff	Std Comb Dev
529.373289	1	C30H49N4O4	529.374832	2.9	1575.0	8.5	ok	even	54.8	108.8	n.a.	n.a.	n.a.	n.a.

HRMS of **5**

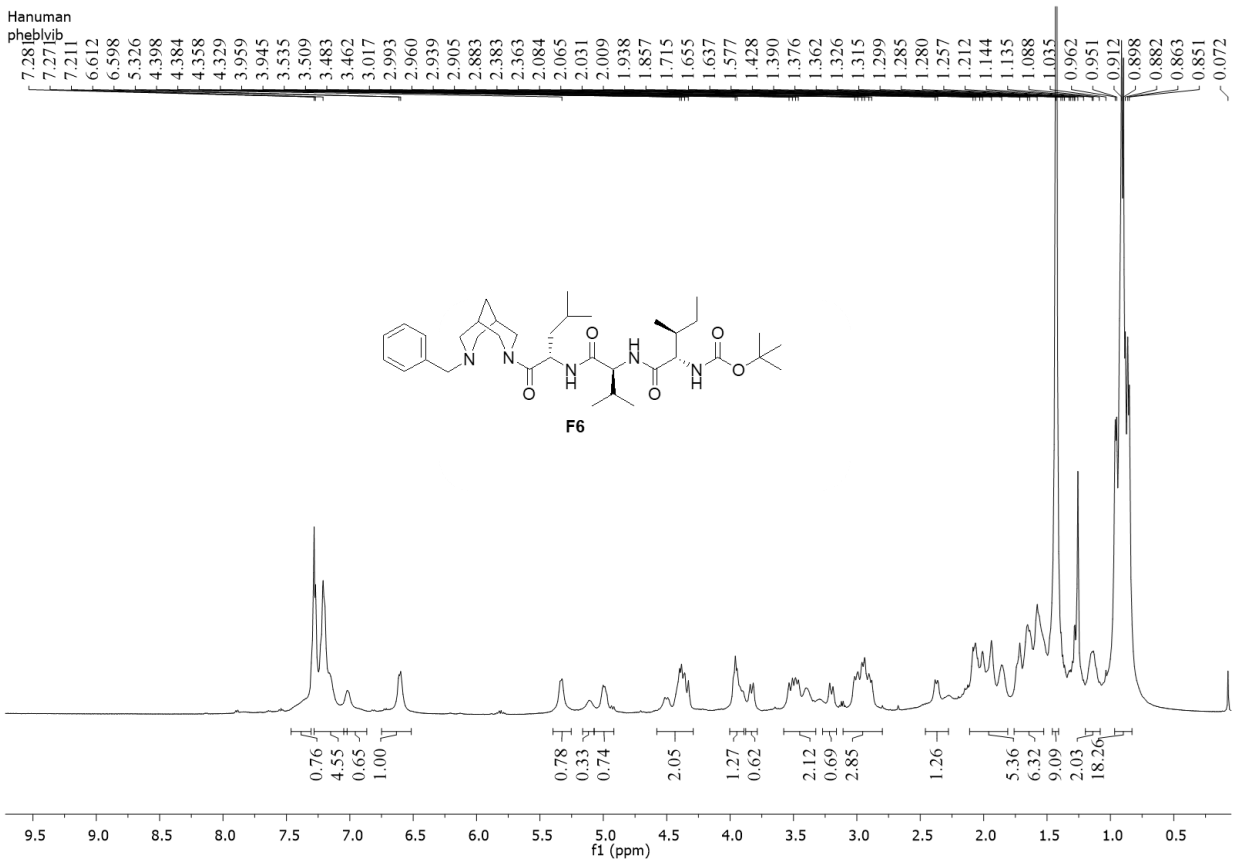

^{1}H NMR ($CDCl_3$, 500 MHz) of **F6**

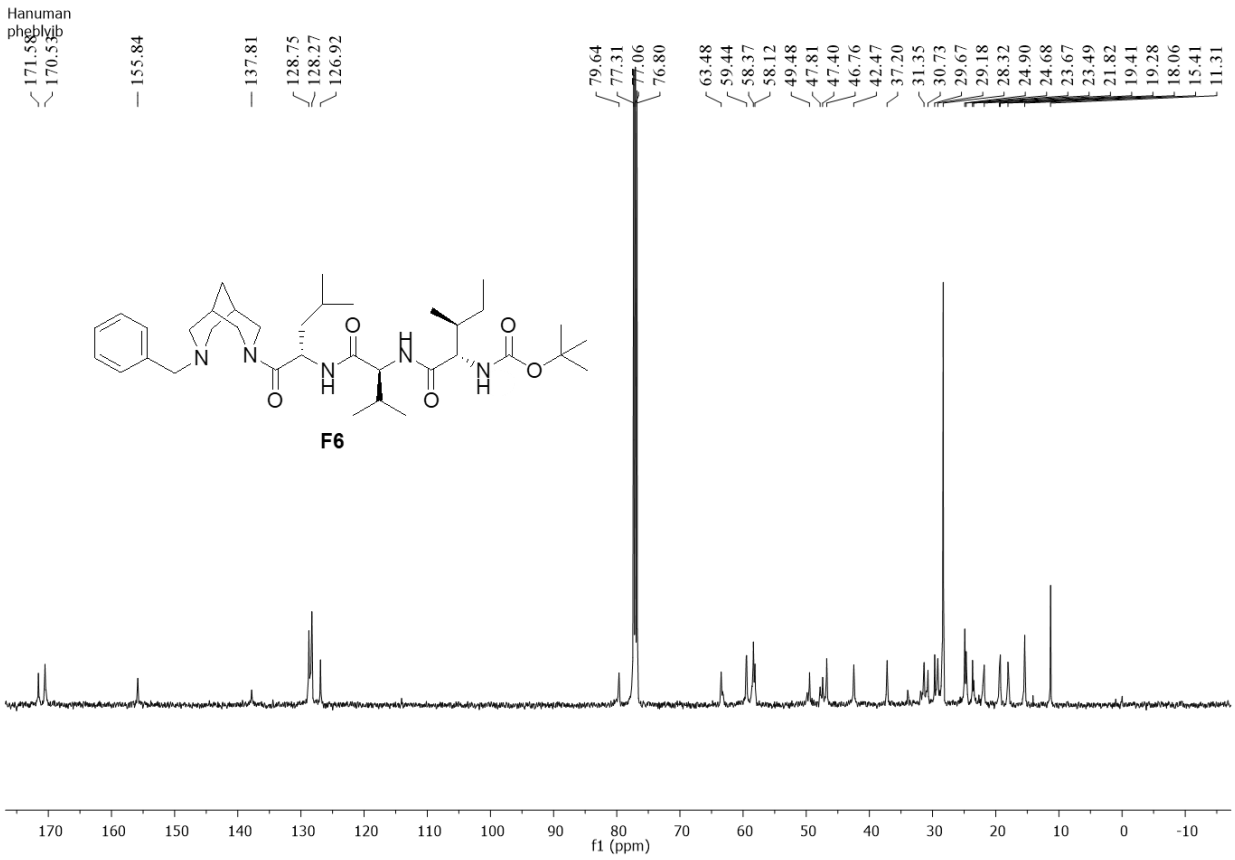

^{13}C NMR (125 MHz, $CDCl_3$) of **F6**

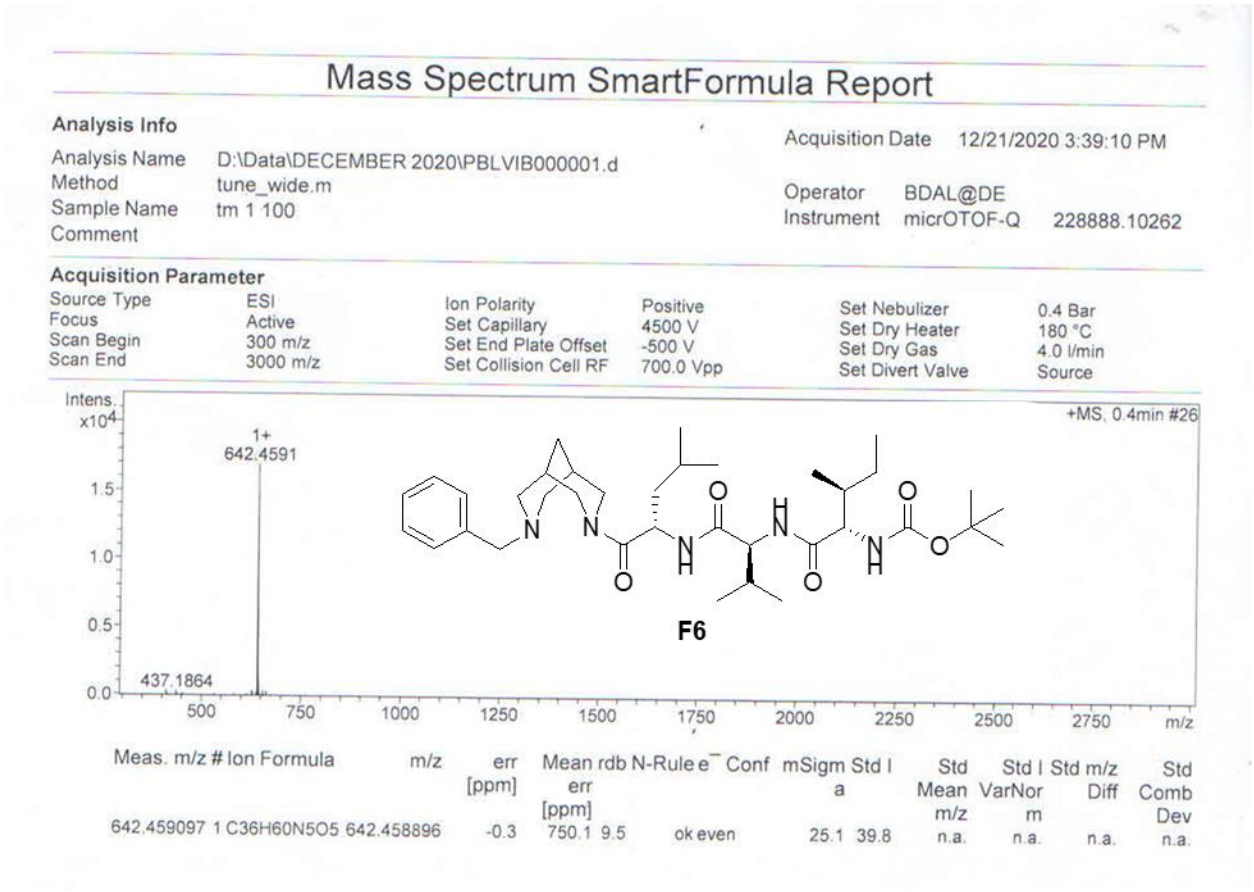
Mass Spectrum SmartFormula Report
Analysis Info
Analysis Name D:\Data\DECEMBER 2020\PBLVIB000001.d
Method tune_wide.m
Sample Name tm 1 100
Comment
Acquisition Date 12/21/2020 3:39:10 PM
Operator BDAL@DE
Instrument micrOTOF-Q 228888.10262
Acquisition Parameter
Source Type ESI
Focus Active
Scan Begin 300 m/z
Scan End 3000 m/z
Ion Polarity Positive
Set Capillary 4500 V
Set End Plate Offset -500 V
Set Collision Cell RF 700.0 Vpp
Set Nebulizer 0.4 Bar
Set Dry Heater 180 °C
Set Dry Gas 4.0 l/min
Set Divert Valve Source
Intens.
x10^4
+MS, 0.4min #26
1+
642.4591
437.1864
F6
m/z
Meas. m/z # Ion Formula m/z err [ppm] Mean err [ppm] rdb N-Rule e¯ Conf mSigma Std I Std Mean m/z Std I VarNorm Std m/z Diff Std Comb Dev
642.459097 1 C36H60N5O5 642.458896 -0.3 750.1 9.5 ok even 25.1 39.8 n.a. n.a. n.a. n.a.

HRMS of **F6**

References:

1 V. Haridas, S. Sadanandan, Y. K. Sharma, S. Chinthalapalli, A. Shandilya, *Tetrahedron Letters* 2012, **53**, 623–626.

2 D. S. Wishart, B. D. Sykes, F. M. Richards, *Biochemistry* 1992, **31**, 1647–1651.

3 The PyMOL Molecular Graphics System, Version 2.0 Schrödinger, LLC.

4 K. Vanommeslaeghe, A. D. MacKerell, *J. Chem. Inf. Model.* 2012, **52**, 3144–3154.

5 M. J. Abraham, T. Murtola, R. Schulz, S. Páll, J. C. Smith, B. Hess, E. Lindahl, *SoftwareX* 2015, *1–2*, 19–25.

6 J. Huang, A. D. MacKerell, *J. Comput. Chem.* 2013, **34**, 2135–2145.

7 V. Zoete, M. A. Cuendet, A. Grosdidier, O. Michielin, *J. Comput. Chem.* 2011, **32**, 2359–2368.

8 F. Neese, *WIREs Comput Mol Sci* 2018, **8**, DOI 10.1002/wcms.1327.